Research Square

Preprints are preliminary reports that have not undergone peer review.
They should not be considered conclusive, used to inform clinical practice,
or referenced by the media as validated information.

The Key Vitamin A Regulator RBP1 Modulates Malignant Biological Behaviors in Head and Neck Squamous Cell Carcinoma

Ji-Ao Zhang
Fourth Hospital of Hebei Medical University
Zifeng Cui
Fourth Hospital of Hebei Medical University
Tiejun Liu
Fourth Hospital of Hebei Medical University
Yueting Lu
Fourth Hospital of Hebei Medical University
Hualin Lu
Fourth Hospital of Hebei Medical University
Hongyue Shang
Fourth Hospital of Hebei Medical University
Bo Dong
Fourth Hospital of Hebei Medical University
Taoran Wang
Fourth Hospital of Hebei Medical University
Manman Yao
49103567@hebmu.edu.cn

Fourth Hospital of Hebei Medical University

Research Article

Keywords: RBP1, HNSCC, vitamin A, proliferation, migration, invasion, immunity, chemoresistance

Posted Date: September 25th, 2026

DOI: https://doi.org/10.21203/rs.3.rs-10690990/v1

License: This work is licensed under a Creative Commons Attribution 4.0 International License.
Read Full License

Additional Declarations: No competing interests reported.

The Key Vitamin A Regulator RBP1 Modulates Malignant Biological Behaviors in Head and Neck Squamous Cell Carcinoma

Authors：
Ji-Ao Zhang,
(Aff1: The Fourth Hospital of Hebei Medical University , Aff2: Hebei Medical University),China <790992952@qq.com>
Zifeng Cui,
(Aff: The Fourth Hospital of Hebei Medical University) , China <cuizifeng358@foxmail.com>
Tiejun Liu,
(Aff: The Fourth Hospital of Hebei Medical University),China <47300561@hebmu.edu.cn>
Yueting Lu,
(Aff: The Fourth Hospital of Hebei Medical University),China <48901999@hebmu.edu.cn>
Hualin Lu,
(Aff: The Fourth Hospital of Hebei Medical University),China <595073285@qq.com>
Hongyue Shang,
(Aff: The Fourth Hospital of Hebei Medical University) , China <845884912@qq.com>
Bo Dong,
(Aff: The Fourth Hospital of Hebei Medical University), China <11634251071@163.com>
Taoran Wang,
(Aff1: The Fourth Hospital of Hebei Medical University , Aff2: Hebei Medical University),China <Wangtaoran2000@163.com>
Manman Yao,
(Aff: The Fourth Hospital of Hebei Medical University),China <49103567@hebmu.edu.cn>

Corresponding Authors:

1.Manman Yao,
(Aff: The Fourth Hospital of Hebei Medical University),China<49103567@hebmu.edu.cn>
2.Tiejun Liu,
(Aff: The Fourth Hospital of Hebei Medical University),China<47300561@hebmu.edu.cn>

Abstract

Background: Head and neck squamous cell carcinoma (HNSCC) ranks as the sixth most common malignancy globally. The involvement of vitamins in carcinogenesis has attracted growing research interest, with vitamin A (retinol) being extensively implicated in cancer biology. Mounting evidence suggests that dysregulated expression of retinol-binding proteins profoundly impacts tumor initiation and progression by compromising retinoid signaling integrity within the tumor microenvironment (TME). Cellular retinol-binding protein 1 (RBP1, also known as CRBP1), a critical modulator of intracellular retinol metabolism in the retinoid family, is primarily responsible for retinol trafficking and metabolic processing. Although RBP1 has been characterized in multiple cancer types and is closely associated with vitamin A homeostasis, its mechanistic role in HNSCC pathogenesis and its regulatory effects on malignant cellular phenotypes remain elusive.

Objectives: This study aimed to systematically investigate the pathogenic mechanisms of HNSCC and to evaluate the potential of RBP1 as a novel molecular target driving HNSCC development and progression. These findings may provide a foundation for developing effective early diagnostic biomarkers and targeted therapeutic strategies for HNSCC.

Methods

Publicly available head and neck squamous cell carcinoma (HNSCC) transcriptomic and clinical datasets were retrieved from The Cancer Genome Atlas (TCGA) database. Differentially expressed protein-coding genes associated with poor prognosis were identified through bioinformatics screening. In parallel, RNA sequencing (RNA-seq) was performed on three paired tissue specimens (tumor and adjacent non-tumor) from HNSCC patients. Genes involved in vitamin A (retinol) metabolism and signaling were curated from the GeneCards database. The intersection of these four gene sets—TCGA-derived prognostic genes, RNA-seq differentially expressed genes, vitamin A-associated genes, and protein-coding genes—was computed to identify candidate molecules. Cellular retinol-binding protein 1 (RBP1, also known as CRBP1) emerged as the most significantly correlated gene with HNSCC and was associated with unfavorable prognosis.The mRNA and protein expression levels of RBP1 were quantified across HNSCC cell lines by quantitative real-time polymerase chain reaction (qRT-PCR) and Western blot analysis, respectively. Based on endogenous RBP1 expression profiles, appropriate HNSCC cell lines were selected for subsequent functional investigations.A retrospective cohort comprising 63 HNSCC patients was enrolled, with paired tumor and adjacent normal tissue specimens and comprehensive clinical metadata collected. RBP1 protein expression was assessed by immunohistochemistry (IHC). Univariate and multivariate Cox regression analyses were conducted on both TCGA cohort data and the 63-patient clinical dataset to evaluate the association between RBP1 expression and malignant phenotypes as well as overall survival outcomes.Gain- and loss-of-function models were established through RBP1 overexpression using the pcDNA3.1 vector and short interfering RNA (siRNA)-mediated knockdown in selected HNSCC cell lines. Functional assays were performed as follows: Cell Counting Kit-8 (CCK-8) assay and colony formation assay for proliferative capacity; wound healing assay for migratory potential; and Transwell chamber assay (with or without Matrigel coating) for invasive capability.Drug resistance analysis was performed using R software and the Gene Expression Profiling Interactive Analysis (GEPIA) platform to investigate the correlation between RBP1 expression and chemoresistance in HNSCC. Tumor immune infiltration patterns were analyzed via the Tumor Immune Estimation Resource (TIMER) database to evaluate RBP1-associated immune microenvironment landscapes in HNSCC.

Results

Quantitative real-time polymerase chain reaction (qRT-PCR) and Western blot analysis demonstrated that cellular retinol-binding protein 1 (RBP1, also known as CRBP1) expression was significantly elevated in head and neck squamous cell carcinoma (HNSCC) cell lines compared with normal head and neck epithelial cell lines. Immunohistochemistry (IHC) revealed markedly higher RBP1 protein levels in HNSCC tumor tissues than in adjacent normal tissues.

Clinical correlation analysis of The Cancer Genome Atlas (TCGA) data indicated that regional lymph node metastasis (N stage) and age were significantly associated with RBP1 expression ($P < 0.05$). Univariate Cox regression analysis identified primary tumor size and local extent (T stage), regional lymph node metastasis (N stage), and high RBP1 expression as predictors of poor prognosis in HNSCC patients ($P < 0.05$). Variables with $P < 0.05$ in the univariate analysis were subsequently entered into multivariate Cox regression analysis, which confirmed that high RBP1 expression served as an independent prognostic factor for unfavorable outcomes in HNSCC.

Analysis of the 63-patient clinical cohort revealed significant correlations between RBP1 expression and regional lymph node metastasis (N stage) as well as overall TNM stage ($P < 0.05$). Univariate Cox analysis demonstrated that primary tumor size and local extent (T stage), regional lymph node metastasis (N stage), advanced TNM stage, and high RBP1 expression were associated with poor prognosis ($P < 0.05$). Multivariate Cox analysis of these significant variables identified advanced TNM stage and high RBP1 expression as independent prognostic factors for adverse outcomes in HNSCC patients.

In RBP1-overexpressing (pcDNA3.1-RBP1) SCC-9 cells, proliferative capacity, colony formation efficiency, migratory ability, and invasive potential were significantly enhanced ($P < 0.001$). Conversely, in RBP1-knockdown (siRNA-RBP1) SCC-25 cells, these malignant phenotypes were markedly attenuated ($P < 0.001$).

Bioinformatics analysis using R software (version 4.4.2) and the Gene Expression Profiling Interactive Analysis (GEPIA) platform revealed a significant correlation between elevated RBP1 expression and paclitaxel resistance in HNSCC, which was further associated with unfavorable prognosis.

Tumor immune infiltration analysis via the Tumor Immune Estimation Resource (TIMER 2.0) database demonstrated that RBP1 expression was significantly associated with the infiltration levels of B cells, CD4+ T cells, CD8+ T cells, dendritic cells, M2 macrophages, mast cells, monocytes, tumor-associated macrophages (TAMs), T follicular helper (Tfh) cells, T helper 1 (Th1) cells, and T helper 2 (Th2) cells, as well as immune checkpoint molecules. Notably, RBP1 exhibited a negative regulatory role in these immune interactions ($P < 0.05$).

Conclusion

Cellular retinol-binding protein 1 (RBP1, also known as CRBP1), a critical regulator of vitamin A (retinol) metabolism, is significantly upregulated in head and neck squamous cell carcinoma (HNSCC) tissues and cell lines. Elevated RBP1 expression is clinically correlated with aggressive malignant phenotypes, including advanced primary tumor size and local extent (T stage), regional lymph node metastasis (N stage), higher overall TNM stage, and patient age, and serves as an independent predictor of unfavorable prognosis. Functional assays demonstrate that RBP1 overexpression (pcDNA3.1-RBP1) promotes proliferative capacity, migratory ability, and invasive potential in HNSCC cells, whereas RBP1 knockdown (siRNA-RBP1) markedly suppresses these malignant behaviors. Furthermore, bioinformatics analysis reveals that RBP1 is significantly associated with paclitaxel resistance and poor clinical outcomes. Notably, RBP1 participates in immune regulation within the HNSCC tumor microenvironment (TME), exerting a negative modulatory effect on antitumor immune responses.

Collectively, these findings establish RBP1 as a valuable biomarker for lymph node metastasis and a potential therapeutic target influencing HNSCC initiation, progression, and prognosis. RBP1 holds considerable promise as a novel early diagnostic biomarker and druggable target for precision management of HNSCC.
Keywords: RBP1; HNSCC; vitamin A; proliferation; migration; invasion; immunity; chemoresistance

Introduction

Head and neck cancer represents the sixth most common malignancy worldwide. According to GLOBOCAN 2020 data, approximately 830,000 new cases and 430,000 deaths are attributed to head and neck squamous cell carcinoma (HNSCC) annually [1]. Although current therapeutic modalities, including surgical resection, radiotherapy, chemotherapy, and multidisciplinary combined treatment strategies, have achieved substantial advances, the 5-year overall survival rate for HNSCC patients remains disappointingly low at 40%–50%, primarily due to tumor recurrence, metastasis, and the emergence of therapeutic resistance [1][2]. Therefore, elucidating the pathogenic mechanisms underlying HNSCC and identifying novel molecular drivers that promote HNSCC initiation and progression hold significant implications for the development of effective early diagnostic biomarkers and targeted therapeutic approaches against this malignancy.

In recent years, with the continuous improvement of living standards, vitamin deficiency has garnered increasing attention. Vitamin A is intimately linked to human health and serves as an essential nutrient in humans, primarily derived from dietary sources. Vitamin A and its bioactive metabolites have long been recognized as critical regulators of epithelial cell proliferation, differentiation, and apoptosis. Vitamin A plays pivotal roles in diverse physiological processes, including vision, immune function, cellular differentiation, and embryonic development [3]. Various natural and synthetic retinoids have also been employed in the treatment of distinct cancer types and dermatological disorders [4]. The efficacy of certain provitamin A carotenoids in scavenging free radicals, eliminating reactive oxygen species, modulating gene expression, and attenuating inflammation both in vitro and in vivo suggests their potential regulatory and preventive effects against metabolic disorders. Concurrently, acting as antioxidants, they can reduce oxidative stress and inflammation, indicating their possible beneficial roles in cancer prevention or therapy. Classical theory posits that retinoic acid (RA), the principal active derivative of vitamin A, exerts tumor-suppressive effects by binding to nuclear retinoic acid receptors (RARs) and retinoid X receptors (RXRs), thereby modulating the transcription of genes associated with cell cycle arrest and differentiation [5][6][7]. However, accumulating evidence indicates that vitamin A exerts bidirectional effects on cancer initiation and progression; under certain conditions, vitamin A and its derivatives may exert procarcinogenic effects, and both excessive and insufficient vitamin A intake may elevate cancer risk [8].

Retinol-binding protein (RBP) serves as the specific transport protein for vitamin A (retinol) in systemic circulation, binding retinol with high affinity and specificity to form an inseparable functional complex. Given that vitamin A is lipophilic and cannot freely dissolve in plasma, RBP increases its solubility approximately 1000-fold through specific binding, thereby maintaining plasma vitamin A concentrations substantially higher than those of the free, unbound state [9]. Cellular retinol-binding protein 1 (RBP1, also known as CRBP1), a 15-kDa cytosolic chaperone protein, functions as a pivotal regulator of intracellular retinol metabolism within the retinoid family and is primarily responsible for retinol trafficking and metabolic processing. RBP1 may exert tissue-specific roles across various malignancies: it acts as a tumor suppressor in breast cancer, ovarian cancer, and other neoplasms

[10][11]; conversely, RBP1 is highly expressed and promotes tumor initiation, progression, and adversely impacts prognosis in head and neck squamous cell carcinoma, oral squamous cell carcinoma, esophageal squamous cell carcinoma, and related malignancies [12][13][14].

Although the functional roles of cellular retinol-binding protein 1 (RBP1, also known as CRBP1) in malignant neoplasms have been progressively elucidated, the precise relationship between vitamin A (retinol) excess or deficiency and tumor initiation and progression remains poorly defined. The expression profile, clinical prognostic value, regulatory network, and impact on neoplastic cellular behaviors of RBP1 in head and neck squamous cell carcinoma (HNSCC) have yet to be fully characterized. The present study was designed to systematically investigate RBP1 expression patterns and clinical significance in HNSCC, elucidate the underlying molecular mechanisms, and further explore the correlation between vitamin A dysregulation and HNSCC pathogenesis. These findings aim to provide novel insights for precise and efficient therapeutic strategies, identify innovative tumor biomarkers and potential therapeutic targets, and advance our understanding of vitamin A-mediated RBP1 regulatory functions in HNSCC.

Materials and Methods

1. Experimental Materials

1.1 Cell Lines

The human normal gingival epithelial cell line HGE and head and neck squamous cell carcinoma (HNSCC) cell lines HSC-3, SCC-9, SCC-25, and CAL-27 were routinely cryopreserved in the Biobank of the Fourth Hospital of Hebei Medical University.

Short interfering RNA (siRNA) targeting RBP1 (siRBP1) was transfected into SCC-25 cells to establish siRBP1-SCC-25 knockdown cell lines. The siRNA sequences (Hippobiotec Co., Ltd.) are detailed in Table 1.

Table1 Sequences of siRNA（RBP1）

RBP1	siRNA sequence（5′-3′）
siRNA-1	S:GAGGAUCUGACAGGCAUAGAUdTdT
	AS: AUCUAUGCCUGUCAGAUCCUCdTdT
siRNA-2	S:GAUGUUGGUCAACGAGAAUUUdTdT
	AS: AAAUUCUCGUUGACCAACAUCdTdT
siRNA-3	S: UGUGGUCUGCAAGCAAGUAUUdTdT
	AS: AAUACUUGCUUGCAGACCACAdTdT

S:Sense; AS:Antisense.

The pcDNA3.1-RBP1 overexpression plasmid was transfected into SCC-9 cells to establish pcDNA3.1-RBP1-SCC-9 overexpression cell lines.

Cell culture conditions: HGE, HSC-3, SCC-9, SCC-25, and CAL-27 cell lines were maintained in high-glucose Dulbecco's Modified Eagle Medium (DMEM) (Servicebio) supplemented with 5% fetal bovine serum (FBS) (Aspen Biotechnology) and 0.5% penicillin-streptomycin (Aspen Biotechnology). Cells were incubated at 37°C in a humidified atmosphere containing 5% CO_2.

1.2 Clinical Tissue Specimen Collection

Paired tumor specimens and adjacent normal tissues (located ≥3 cm from the tumor margin) were collected from HNSCC patients who underwent surgical resection at the Department of Oral and Maxillofacial Surgery, Fourth Hospital of Hebei Medical University, between May 2015 and December 2019.**Inclusion criteria:** (i) pathologically confirmed HNSCC; (ii) age ≥18 years; (iii)

complete tumor staging data.**Exclusion criteria:** (i) prior diagnosis of HNSCC with previous treatment; (ii) concurrent malignancy at other anatomical sites; (iii) incomplete clinical documentation; (iv) compromised hematological or immune system; (v) psychiatric disorders.Postoperative follow-up was conducted until December 31, 2024. Overall survival (OS) was defined as the interval from pathological diagnosis to death from any cause or the last follow-up date, whichever occurred first. This study was approved by the Ethics Committee of the Fourth Hospital of Hebei Medical University. Written informed consent was obtained from all patients or their legally authorized representatives.

2. Experimental Methods

2.1 Cell Counting Kit-8 (CCK-8) Assay

HNSCC cells subjected to transfection and subsequent 24-hour culture were harvested by trypsinization. Experimental and control groups were seeded into 96-well plates at a density of 1,000 cells per well, with five replicate wells per group. Peripheral wells of the 96-well plate were filled with phosphate-buffered saline (PBS) to minimize evaporation-induced experimental variation. Plates were returned to the incubator for continuous culture. Cell proliferation was assessed at five time points: 0, 24, 48, 72, and 96 hours. Prior to detection, CCK-8 reagent was added to each well at a 1:10 dilution (CCK-8 reagent: complete culture medium = 1:9), followed by incubation in a light-protected environment for 2 hours. Absorbance at 450 nm was measured using a microplate reader. Each experiment was performed in triplicate under identical conditions, and the resulting data were compiled to generate proliferation curves. Statistical analysis was performed using two-way repeated measures analysis of variance (ANOVA).

2.2 Colony Formation Assay

1) Cell suspension preparation: Using 6-well plates as an example, RBP1-knockdown or RBP1-overexpressing transiently transfected cells in the logarithmic growth phase were collected. Following trypsinization and centrifugation, the supernatant was aspirated, and cell pellets were resuspended in ice-cold serum-free medium. The suspension was thoroughly pipetted to ensure homogeneous dispersion and then set aside for subsequent use.

2) Cell seeding and culture: Based on cell counting results, cells were seeded at a density of 1,000 cells per well in 2 mL fresh complete culture medium, with two replicate wells per group. After seeding, the plates were gently agitated in a figure-eight motion to ensure uniform cell distribution, then transferred to a 37°C cell culture incubator.

3) Culture maintenance: The culture medium was refreshed every 2 days. Cell growth status was monitored under an inverted microscope, and colony formation as well as the cell number within each colony were documented.

4) Termination criterion: Culture was terminated when the majority of individual colonies contained more than 50 cells under microscopic examination, followed by subsequent processing.

5) Cell fixation: The original culture medium was aspirated from the 6-well plates. Wells were gently rinsed twice with phosphate-buffered saline (PBS), and excess liquid was completely removed. Each well was then treated with 800 μL of 4% paraformaldehyde (PFA) and fixed at room temperature for 20 minutes.

6) Cell staining: The fixative was aspirated, and wells were washed twice with PBS. Each well was subsequently stained with 800 μL of crystal violet solution at room temperature in a light-protected environment for 20 minutes.

7) Image acquisition and data analysis: After removing the staining solution, residual dye was removed by rinsing with PBS. The plates were inverted onto absorbent paper and air-dried. Images

were captured for documentation. ImageJ software was employed for image processing, and colony numbers were quantified to generate bar graphs. Statistical analysis: Overall significance was assessed by one-way analysis of variance (ANOVA), followed by multiple comparisons using Tukey's honestly significant difference (HSD) post-hoc test.

2.3 Wound Healing Assay

HNSCC cells successfully transfected for 24 hours and reaching 85%–90% confluence were utilized. A straight scratch was generated perpendicular to the plate bottom using a sterile 200 μL pipette tip along a ruler, ensuring consistent scratch width and length across all groups to minimize experimental variation. Cellular debris was removed by gently washing with phosphate-buffered saline (PBS) 2–3 times. Subsequently, 2 mL serum-free Dulbecco's Modified Eagle Medium (DMEM) was added to each well. Phase-contrast images of the scratch area were captured at 0 hours using an inverted microscope. Plates were then returned to the incubator for continuous culture, and scratch closure was documented photographically under identical conditions at 24 hours. The relative wound area was quantified using ImageJ software by measuring the scratch width at three predefined points per well, and the percentage of wound closure was calculated as follows: [(scratch width at 0 h − scratch width at 24 h) / scratch width at 0 h] × 100%. Each experiment was performed in triplicate under identical conditions, and quantitative data were compiled to generate bar graphs. Statistical analysis: Overall significance was assessed by one-way analysis of variance (ANOVA), followed by multiple comparisons using Tukey's honestly significant difference (HSD) post-hoc test.

2.4 Transwell Invasion Assay

Ice-cold serum-free medium was mixed with Matrigel basement membrane matrix at a dilution ratio of 8:1. Transwell chambers (24-well format) were placed into the plate, and 100 μL of the diluted Matrigel solution was carefully and evenly dispensed onto the upper surface of the Transwell membrane using a pipette tip. The procedure was performed meticulously to ensure complete coverage of the membrane without bubble formation. The 24-well plate was transferred to the incubator for 2 hours to allow gel polymerization. HNSCC cells successfully transfected for 24 hours were harvested by trypsinization and seeded onto the upper chamber at a density of 8×10^4 cells per well in 200 μL serum-free medium. The lower chamber was filled with 600 μL complete medium supplemented with 10% fetal bovine serum (FBS) as a chemoattractant. Cells were incubated for 16 hours to permit invasion through the Matrigel-coated membrane.Following incubation, the medium was aspirated from both chambers. Non-invading cells on the upper membrane surface were gently removed using a cotton swab. The Transwell inserts were then washed twice with phosphate-buffered saline (PBS). The inserts were fixed in 2–4 mL 4% paraformaldehyde (PFA) for 20 minutes at room temperature. After fixation, the PFA solution was aspirated, and the inserts were washed twice with PBS. Subsequently, crystal violet solution was added to the inserts for 10-minute staining at room temperature in a light-protected environment. Excess stain was removed by washing twice with PBS. The inserts were air-dried at room temperature.For image acquisition, random fields per insert were captured under an inverted microscope using bright-field illumination. Invading cells on the lower membrane surface were quantified using ImageJ software. Each experiment was performed in triplicate under identical conditions, and the resulting data were compiled to generate bar graphs. Statistical analysis: Overall significance was assessed by one-way analysis of variance (ANOVA), followed by multiple comparisons using Tukey's honestly significant difference (HSD) post-hoc test.

2.5 Western Blot Analysis

Cell lysis buffer was prepared by mixing radioimmunoprecipitation assay (RIPA) buffer (GLPBIO) and phenylmethylsulfonyl fluoride (PMSF) protease inhibitor (Servicebio) at a ratio of 100:1. Cells were lysed on ice for 30 minutes. Following complete lysis, samples were centrifuged at 12,000 rpm for 15 minutes at 4°C. The supernatant was collected, and protein concentration was determined using the bicinchoninic acid (BCA) assay kit. Sodium dodecyl sulfate-polyacrylamide gel electrophoresis (SDS-PAGE) gels were prepared using a Western blot gel preparation kit (Servicebio). Protein samples were subjected to electrophoresis under constant cooling at 200 mA for 20 minutes followed by 350 V for 40 minutes. Electrophoretic transfer to polyvinylidene difluoride (PVDF) membranes was performed under ice-cooled conditions.Membranes were blocked with skim milk at room temperature for 1 hour, then washed three times with Tris-buffered saline containing 0.1% Tween-20 (TBST). Primary antibodies were applied, and membranes were incubated overnight at 4°C. The following day, membranes were washed three times with TBST, followed by incubation with secondary antibodies at room temperature for 1 hour. After secondary antibody incubation, membranes were washed three times with TBST. Protein bands were visualized by enhanced chemiluminescence (ECL) detection. Image annotation and format standardization were performed using Adobe Photoshop software.

2.6 Quantitative Real-Time Polymerase Chain Reaction (qRT-PCR)

Total RNA was extracted using the Trizol reagent method (SimGen), reverse-transcribed into complementary DNA (cDNA), and subsequently subjected to qRT-PCR amplification on a real-time fluorescence quantitative PCR instrument. Glyceraldehyde-3-phosphate dehydrogenase (GAPDH) served as the internal reference gene, and relative expression levels were calculated using the 2^(-ΔΔCt) method. Each group was performed in triplicate with three technical replicate wells, and each experiment was repeated three times independently. Primer sequences are detailed in Table 2.The reaction mixture comprised a total volume of 10 μL: 3.6 μL RNase-free water, 5 μL SYBR Green Mix, 0.2 μL forward primer, 0.2 μL reverse primer, and 1 μL template cDNA. The qRT-PCR assay kit (Nearshore Biotech) was utilized for all reactions.The thermal cycling conditions were: initial denaturation at 95°C for 10 minutes; followed by 40 cycles of denaturation at 95°C for 15 seconds, annealing at 60°C for 30 seconds, and extension at 72°C for 30 seconds; with a final melting curve analysis stage of 95°C for 15 seconds, 60°C for 1 minute, and 95°C for 15 seconds.

Table2 Primers of qRT-PCR(RBP1)

Gene	Sequences(5′-3′)
GAPDH-F	GAAGGTGAAGGTCGGAGTC
GAPDH-R	GAAGATGGTGATGGGATTTC
RBP1-F	TTGCTCAGTCAAGGGTCAGT
RBP1-R	CCCAACATTATGTGCTGGGC

F:Forward primer; R:Reverse primer.

2.7Immunohistochemical evaluation:

Cytoplasmic yellow or brown granular staining was considered positive, whereas nuclear and membranous non-specific staining was excluded. Unstained cells were regarded as negative. All slides were evaluated independently by two experienced pathologists who were blinded to the clinical and pathological data. Discrepancies were resolved by consensus discussion. A semi-quantitative scoring system was applied. Five high-power fields (×400 magnification) were randomly selected, and approximately 100 cells per field were counted to obtain the average. The proportion of positive cells was scored into four grades: 0 (≤10%), 1 (11–30%), 2 (31–60%), or 3 (≥60%). A score >0 was defined as positive staining. Samples were subsequently categorized into RBP1 high-expression (≥ median) and

low-expression (< median) groups based on the median score, with the median value assigned to the high-expression group.

3. Statistical Analysis

Experimental data were compiled, analyzed, and visualized using R software (version 4.4.2), GraphPad Prism (version 9.5.1), IBM SPSS Statistics (version 16.0), Tumor Immune Estimation Resource (TIMER 2.0), Gene Expression Profiling Interactive Analysis 3 (GEPIA3), ImageJ (version 1.53), and Adobe Photoshop. Statistical methods included Cox regression analysis, one-way analysis of variance (ANOVA), two-way ANOVA, followed by multiple comparisons using Tukey's honestly significant difference (HSD) post-hoc test, as appropriate for specific experimental designs.

Results

1. Gene Screening

Cellular retinol-binding protein 1 (RBP1, also known as CRBP1) was identified as a protein potentially exerting critical effects on head and neck squamous cell carcinoma (HNSCC) progression. We initially performed RNA sequencing (RNA-seq) on three paired HNSCC tissue specimens and simultaneously retrieved HNSCC transcriptomic data from The Cancer Genome Atlas (TCGA) database. Analysis of 522 HNSCC tissues and 44 normal tissues from TCGA yielded 958 differentially expressed genes (668 upregulated and 290 downregulated; screening criteria: $|\log_2$ fold change (logFC)$| > 2$, adjusted *P* value (*P*.adj) < 0.001) (Fig. 1a, b). Parallel analysis of our laboratory RNA-seq data from three paired HNSCC samples identified 457 differentially expressed genes (265 upregulated and 192 downregulated; screening criteria: $|\text{logFC}| > 2$, *P*.adj < 0.001) (Fig. 1c, d).

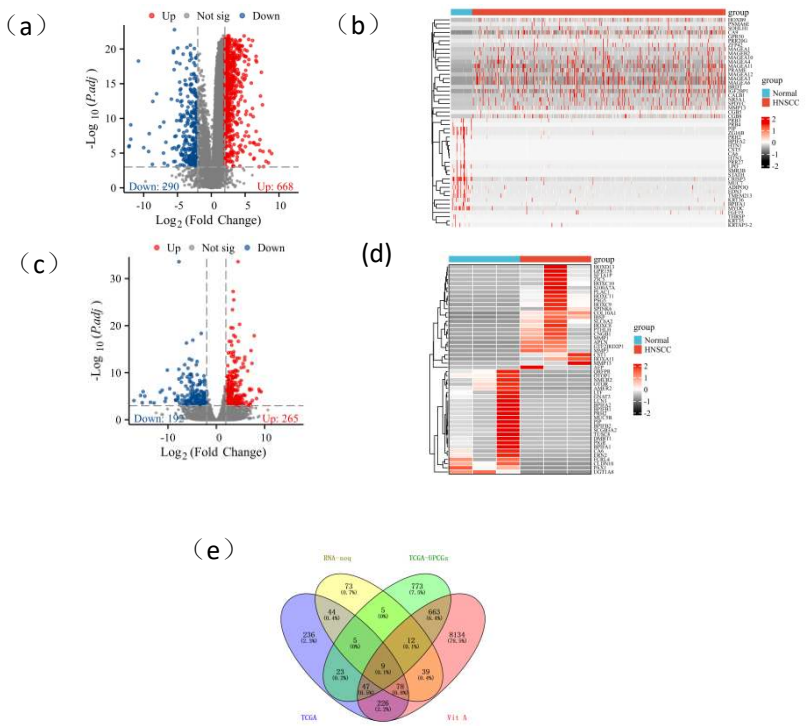


Fig.1 Differential Expression Analysis and Target Gene Screening.(a) Volcano plot of differentially expressed genes in The Cancer Genome Atlas (TCGA) head and neck squamous cell carcinoma (HNSCC). Red, upregulated (668); blue, downregulated (290) (log_2 fold change [logFC] > 2, adjusted *P* value [*P*.adj] < 0.001).**(b)** Heatmap of top 25 upregulated and top 25 downregulated genes by fold change in TCGA-HNSCC.**(c)** Volcano plot of differentially expressed genes in laboratory RNA sequencing (RNA-seq). Red, upregulated (265); blue, downregulated (192) (logFC > 2, *P*.adj < 0.001).**(d)** Heatmap of top 25 upregulated and top 25 downregulated genes by fold change in laboratory RNA-seq.**(e)** Venn diagram of four gene sets: 668 upregulated genes from TCGA-HNSCC (logFC > 2, *P*.adj < 0.001), 265 upregulated genes from three paired HNSCC tissue RNA-seq (logFC > 2, *P*.adj < 0.001), 1,537 poor-prognosis protein-coding genes from TCGA identified by Cox regression analysis (hazard ratio [HR] > 1, *P* < 0.05), and 9,208 vitamin A (retinol)-associated genes retrieved from the GeneCards database. Intersection: 9 candidate genes.

Following exclusion of samples with incomplete clinical information from the 522 TCGA-HNSCC patients, 503 cases remained eligible for subsequent survival analysis. Cox regression analysis of the curated cohort identified 1,537 protein-coding genes associated with poor prognosis (hazard ratio [HR] > 1, *P* < 0.05). Concurrently, 9,208 vitamin A (retinol)-associated genes were retrieved from the GeneCards database. Intersection analysis of four gene sets—668 upregulated genes from TCGA-HNSCC, 265 upregulated genes from the three-paired HNSCC RNA-seq dataset, 1,537 poor-prognosis protein-coding genes from TCGA, and 9,208 vitamin A-associated genes from GeneCards—yielded nine preliminary candidate genes (Fig. 1e): RBP1, CAV1, FAP, HMGA2, PDPN, PLAU, STC2, TGFBI, and ULBP2. Kaplan-Meier (KM) survival analysis with visualization was subsequently performed for each candidate gene, confirming that all exhibited statistically significant associations with unfavorable prognosis (HR > 1, *P* < 0.05), indicating that elevated expression levels

correlated with poorer survival outcomes (Fig. 2). Through systematic literature review, RBP1 was identified as being intimately linked to vitamin A biology and functioning as a critical modulator within the retinoid metabolic pathway. Given that the mechanistic role of RBP1 in HNSCC pathogenesis has yet to be fully characterized, RBP1 was ultimately selected as the target gene for the present investigation.

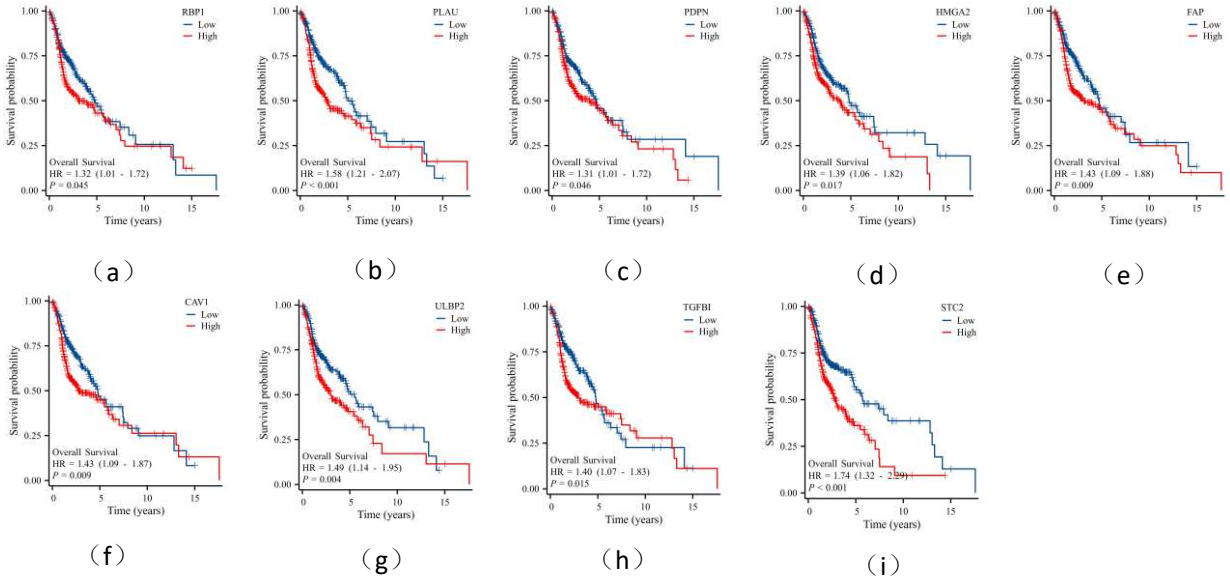


Fig.2 Kaplan-Meier (KM) Survival Analysis of Intersection Genes.(a) RBP1; **(b)** CAV1; **(c)** FAP; **(d)** HMGA2; **(e)** PDPN; **(f)** PLAU; **(g)** STC2; **(h)** TGFBI; **(i)** ULBP2.All nine genes.exhibited significant associations with poor prognosis (hazard ratio [HR] > 1, $P < 0.05$), with elevated expression correlating with reduced overall survival.

2. Pan-Cancer Analysis and Receiver Operating Characteristic (ROC) Diagnostic Curve

Pan-cancer analysis of RBP1 was performed using TIMER 2.0. Among 32 cancer types, RBP1 was significantly upregulated in 10/32 malignancies: bladder urothelial carcinoma (BLCA), glioblastoma multiforme (GBM), head and neck squamous cell carcinoma (HNSCC), kidney renal clear cell carcinoma (KIRC), kidney renal papillary cell carcinoma (KIRP), liver hepatocellular carcinoma (LIHC), lung adenocarcinoma (LUAD), lung squamous cell carcinoma (LUSC), prostate adenocarcinoma (PRAD), and stomach adenocarcinoma (STAD) (Fig. 3a). These findings further substantiate the potential of RBP1 as a novel molecular marker for early diagnosis, prognostic evaluation, and targeted therapeutic strategies in HNSCC.

Receiver operating characteristic (ROC) curve analysis was subsequently employed to evaluate the diagnostic performance of RBP1 in distinguishing HNSCC from normal tissues. The area under the ROC curve (AUC) was 0.886 (95% confidence interval [CI]: 0.844–0.927), indicating robust discriminatory capacity between malignant and normal groups and confirming the high reliability of RBP1 as a diagnostic risk indicator for HNSCC (Fig. 3b).

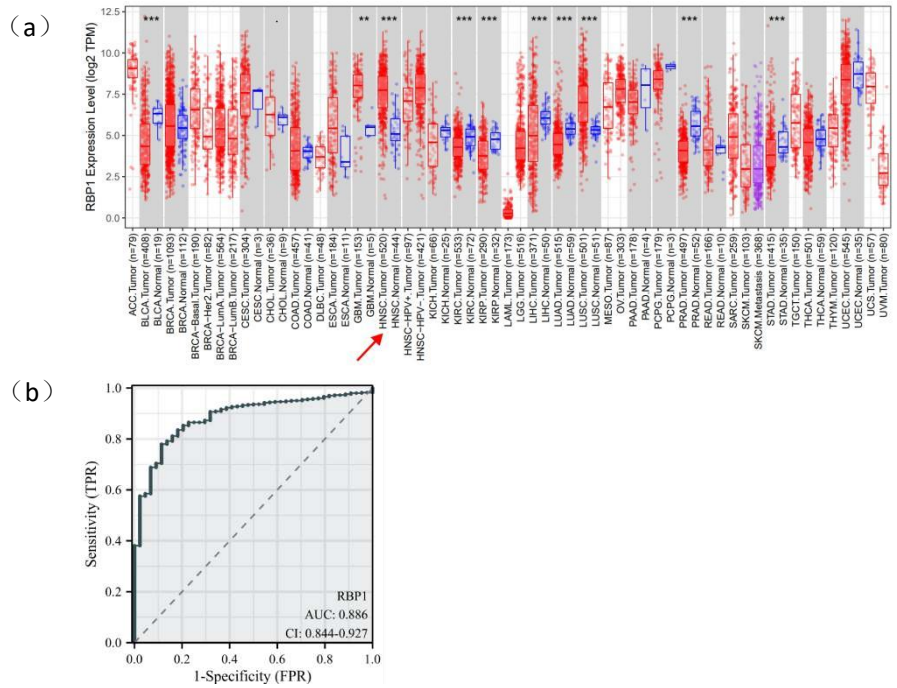


Fig.3 Pan-Cancer Analysis of RBP1 and Receiver Operating Characteristic (ROC) Diagnostic Curve in HNSCC.(a) Pan-cancer analysis of RBP1 expression across multiple malignancies using TIMER 2.0.**(b)** ROC curve of RBP1 for HNSCC diagnosis. Area under the curve (AUC): 0.886 (95% confidence interval [CI]: 0.844–0.927).

3. Clinical Correlation Analysis

Following exclusion of cases with incomplete clinical information from the TCGA dataset, HNSCC patients were stratified into low and high RBP1 expression groups based on the median expression value, yielding 183 cases in the low-expression group and 187 cases in the high-expression group. Clinical correlation analysis revealed significant associations between RBP1 expression and regional lymph node metastasis (N stage) as well as age (Table 3).

Table 3. Correlation Between RBP1 Expression and Clinicopathological Characteristics in HNSCC Patients from The Cancer Genome Atlas (TCGA) Database

Characteristics	Low expression of RBP1	High expression of RBP1	*P* value
n	183	187	
T stage, n (%)			0.715
T1&T2	59 (15.9%)	57 (15.4%)	
T3&T4	124 (33.5%)	130 (35.1%)	
N stage, n (%)			**0.048***
N0	102 (27.6%)	85 (23%)	
N1&N2&N3	81 (21.9%)	102 (27.6%)	

Characteristics	Low expression of RBP1	High expression of RBP1	*P* value
Stage, n (%)			0.717
Stage I&Stage II	40 (10.8%)	38 (10.3%)	
Stage III&Stage IV	143 (38.6%)	149 (40.3%)	
Grade, n (%)			0.545
G1&G2	137 (37%)	145 (39.2%)	
G3&G4	46 (12.4%)	42 (11.4%)	
Gender, n (%)			0.824
Female	49 (13.2%)	52 (14.1%)	
Male	134 (36.2%)	135 (36.5%)	
Age, n (%)			**0.007***
<= 60	76 (20.5%)	104 (28.1%)	
> 60	107 (28.9%)	83 (22.4%)	

4. Univariate and Multivariate Cox Regression Analysis of TCGA-HNSCC Data

Univariate Cox regression analysis of TCGA data demonstrated that primary tumor size and local extent (T stage), regional lymph node metastasis (N stage), and high RBP1 expression were significantly associated with unfavorable prognosis in HNSCC patients ($P < 0.05$). Variables with $P < 0.05$ in the univariate analysis were subsequently entered into multivariate Cox regression analysis, which confirmed that high RBP1 expression served as an independent prognostic factor for adverse outcomes in HNSCC patients (Table 4).

Table 4. Univariate and Multivariate Cox Regression Analysis of HNSCC Patients in the TCGA Database

Characteristics	Total	Univariate analysis	Multivariate analysis

		Hazard ratio (95% CI)	*P* value	Hazard ratio (95% CI)	*P* value
Clinical T stage	463				
T1&T2	168	Reference		Reference	
T3&T4	295	1.478 (1.002 - 2.181)	**0.049***	1.359 (0.908 - 2.034)	0.136
Clinical N stage	456				
N0	224	Reference		Reference	
N1&N2&N3	232	1.486 (1.045 - 2.113)	**0.028***	1.404 (0.979 - 2.012)	0.065
Clinical stage	464				
Stage I&Stage II	107	Reference			
Stage III&Stage IV	357	1.161 (0.759 - 1.775)	0.492		
Histologic grade	463				
G1&G2	347	Reference			
G3&G4	116	1.055 (0.715 - 1.557)	0.788		
Gender	478				
Female	123	Reference			
Male	355	0.968 (0.652 - 1.439)	0.874		
Age	478				
<= 60	237	Reference			
> 60	241	1.088 (0.770 - 1.538)	0.632		
RBP1	478				
Low	236	Reference		Reference	
High	242	1.570 (1.104 - 2.233)	**0.012***	1.565 (1.096 - 2.235)	**0.014***

5. Validation of RBP1 Expression and Its Effects on Cellular Biological Functions

Subsequently, we experimentally validated RBP1 expression in HNSCC tissues and cell lines, and investigated its functional impact on neoplastic cellular behaviors.

5.1 RBP1 Expression in HNSCC Tissues

Initially, quantitative real-time polymerase chain reaction (qRT-PCR) was employed to detect RBP1 expression at the mRNA level in normal oral epithelial tissues and head and neck squamous cell carcinoma (HNSCC) specimens. The results demonstrated that RBP1 expression was significantly

elevated in HNSCC compared with adjacent normal tissues ($P < 0.001$) (Fig. 4a). Hematoxylin and eosin (HE) staining was subsequently performed to validate the histopathological identity of the tissue specimens as normal head and neck tissues and HNSCC tissues (Fig. 4b, c). Immunohistochemistry (IHC) was then applied to assess RBP1 protein expression in HNSCC and adjacent normal tissues. The results revealed that RBP1 expression was markedly higher in HNSCC tissues than in adjacent normal counterparts (Fig. 4d–g).

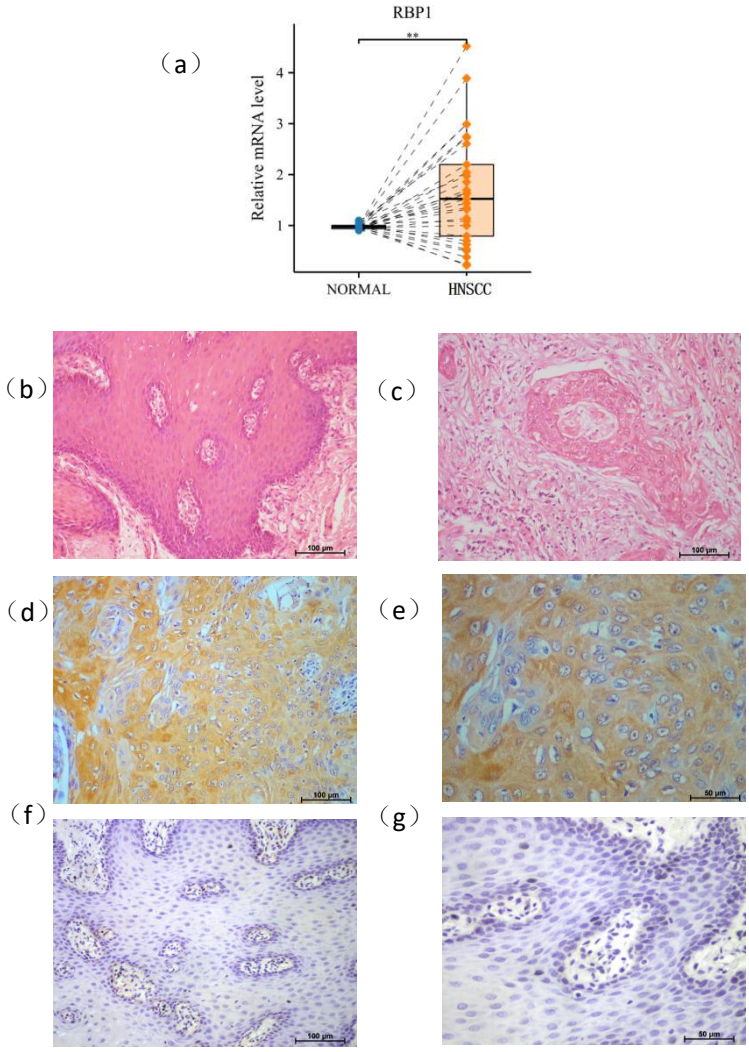


Fig.4 RBP1 Expression in HNSCC Tissues.(a) Quantitative real-time polymerase chain reaction (qRT-PCR) detection of RBP1 mRNA levels in normal oral epithelial tissues and head and neck squamous cell carcinoma (HNSCC) specimens. RBP1 expression was significantly elevated in HNSCC compared with normal tissues ($P < 0.01$).**(b)** Hematoxylin and eosin (HE) staining of adjacent normal tissue (20× magnification).**(c)** HE staining of HNSCC tissue (20× magnification).**(d)** RBP1 immunohistochemistry (IHC) staining in HNSCC tissue (20× magnification).**(e)** RBP1 IHC staining in HNSCC tissue (40× magnification).**(f)** RBP1 IHC staining in adjacent normal tissue (20× magnification).**(g)** RBP1 IHC staining in adjacent normal tissue (40× magnification).

5.2 Clinical Correlation Analysis

Based on immunohistochemistry (IHC) results, the 63 clinical specimens were stratified into high and low RBP1 expression groups, comprising 43 and 20 cases, respectively. Clinical correlation analysis revealed significant associations between RBP1 expression levels and regional lymph node metastasis (N stage) as well as overall TNM stage (Table 5).

Table 5. Correlation Between RBP1 Protein Expression and Clinicopathological Characteristics in 63 HNSCC Patients from the Fourth Hospital of Hebei Medical University

Characteristics	LOW	HIGH	*P value*
n	20	43	
Age, n (%)			1.000
≤60	3 (4.8%)	8 (12.7%)	
＞60	17 (27%)	35 (55.6%)	
Gender, n (%)			0.243
FEMALE	12 (19%)	19 (30.2%)	
MALE	8 (12.7%)	24 (38.1%)	
Grade, n (%)			0.206
G1-G2	18 (28.6%)	31 (49.2%)	
G3-G4	2 (3.2%)	12 (19%)	
T Staging, n (%)			1.000
T1-T2	16 (25.4%)	33 (52.4%)	
T3-T4	4 (6.3%)	10 (15.9%)	
N Staging, n (%)			**0.024***
N0	14 (22.2%)	17 (27%)	
N1-N2-N3	6 (9.5%)	26 (41.3%)	
TNM stage, n (%)			**0.039***
I-II	13 (20.6%)	16 (25.4%)	
III-IV	7 (11.1%)	27 (42.9%)	

5.3 Univariate and Multivariate Cox Regression Analysis of 63 HNSCC Patients from the Fourth Hospital of Hebei Medical University

Univariate Cox regression analysis of the 63-patient clinical cohort demonstrated that primary tumor size and local extent (T stage), regional lymph node metastasis (N stage), overall TNM stage, and high RBP1 expression were significantly associated with unfavorable prognosis ($P < 0.05$). Variables with $P < 0.05$ in the univariate analysis were subsequently entered into multivariate Cox regression analysis, which confirmed that high RBP1 expression and advanced overall TNM stage served as independent prognostic factors for adverse outcomes in HNSCC patients (Table 6).

Table 6. Univariate and Multivariate Cox Regression Analysis of 63 HNSCC Patients from the Fourth Hospital of Hebei Medical University

Characteristics	Total(N)	Univariate analysis		Multivariate analysis	
		Hazard ratio (95% CI)	*P value*	Hazard ratio (95% CI)	*P value*
IHC	63				
LOW	20	Reference		Reference	
HIGH	43	2.817 (1.174 - 6.760)	**0.020***	2.641 (1.030 - 6.769)	**0.043***
Age	63				
≤60	11	Reference			
＞60	52	0.724 (0.296 - 1.772)	0.479		
Gender	63				
Female	31	Reference			
Male	32	1.055 (0.535 - 2.083)	0.877		
Grade	63				
G1-G2	49	Reference			
G3-G4	14	1.140 (0.494 - 2.631)	0.758		
T stage	63				
T1-T2	49	Reference		Reference	
T3-T4	14	2.184 (1.062 - 4.494)	**0.034***	1.612 (0.679 - 3.828)	0.279
N stage	63				
N0	31	Reference		Reference	
N1-N3	32	2.042 (1.013 - 4.118)	**0.046***	0.269 (0.054 - 1.330)	0.107

Characteristics	Total(N)	Univariate analysis		Multivariate analysis	
		Hazard ratio (95% CI)	*P value*	Hazard ratio (95% CI)	*P value*
TNM stage	63				
I-II	29	Reference		Reference	
III-IV	34	2.581 (1.244 - 5.354)	**0.011**	6.622 (1.075 - 40.802)	**0.042***

5.4 RBP1 Expression in HNSCC Cell Lines

Quantitative real-time polymerase chain reaction (qRT-PCR) and Western blot analysis were employed to detect RBP1 expression at both mRNA and protein levels in the human normal gingival epithelial cell line HGE and head and neck squamous cell carcinoma (HNSCC) cell lines (HSC-3, SCC-9, SCC-25, and CAL-27). The results demonstrated that RBP1 expression was significantly elevated in HNSCC cell lines SCC-9, SCC-25, and CAL-27 compared with HGE cells (Fig. 5a, b). Based on these findings, SCC-9 and SCC-25 cell lines were selected for subsequent functional experiments.

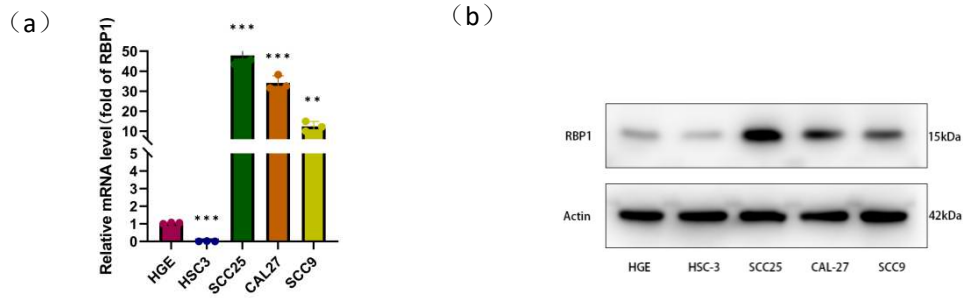


Fig.5 RBP1 Expression in HNSCC Cell Lines.(a) Quantitative real-time polymerase chain reaction (qRT-PCR) detection of RBP1 mRNA levels in HNSCC cell lines (HSC-3, SCC-9, SCC-25, and CAL-27) compared with the human normal gingival epithelial cell line (HGE). RBP1 expression was significantly elevated in SCC-9, SCC-25, and CAL-27 compared with HGE ($P < 0.01$).**(b)** Western blot analysis of RBP1 protein levels in HNSCC cell lines (HSC-3, SCC-9, SCC-25, and CAL-27) compared with HGE. β-actin served as the loading control.

Based on these findings, SCC-9 and SCC-25 cell lines were selected for subsequent functional experiments.

5.5 Establishment of RBP1 Overexpression and Knockdown Models for Functional Assays

5.5.1 Effects of RBP1 Knockdown on Biological Functions of HNSCC Cell Lines

(1) Validation of RBP1 Knockdown and Transfection Efficiency

Following 24-hour transfection of SCC-25 cells, quantitative real-time polymerase chain reaction (qRT-PCR) was performed to assess RBP1 mRNA expression. The results demonstrated that RBP1 expression was significantly reduced in the siRBP1 group (transfected with siRNA-RBP1 silencing vector) compared with the si-NC group (transfected with siRNA negative control vector) (Fig. 6a, $P < 0.001$). Subsequently, SCC-25 cells were harvested at 48 hours post-transfection for Western blot

analysis of RBP1 protein expression. The results confirmed that RBP1 protein levels were markedly decreased in the siRBP1 group compared with the si-NC group (Fig. 6b).siRBP1#1 and siRBP1#2, which exhibited comparable knockdown efficiencies, were selected for subsequent functional experiments.

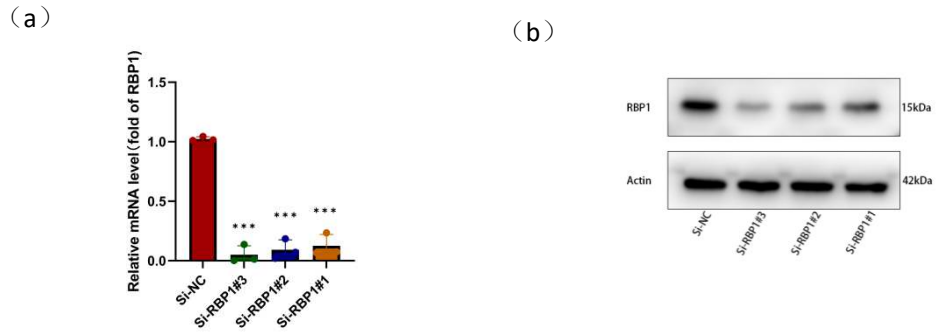


Fig.6 RBP1 Expression Following Knockdown in SCC-25 Cells.(a) Quantitative real-time polymerase chain reaction (qRT-PCR) detection of RBP1 mRNA expression following knockdown in SCC-25 cells. Compared with the si-NC (negative control) group, RBP1 expression was significantly reduced in the si-RBP1#1, si-RBP1#2, and si-RBP1#3 groups ($P < 0.001$).**(b)** Western blot analysis of RBP1 protein expression following knockdown in SCC-25 cells. β-actin served as the loading control.

(2) Effect of RBP1 Knockdown on Proliferative Capacity of SCC-25 Cells

Cell Counting Kit-8 (CCK-8) assay data demonstrated that the absorbance at 450 nm (A_{450}) of SCC-25 cells in the siRBP1 group was significantly reduced compared with the si-NC group following 96-hour culture, with statistically significant differences observed (Fig. 7, $P < 0.001$). These results indicate that RBP1 knockdown suppresses the proliferative capacity of HNSCC SCC-25 cells.

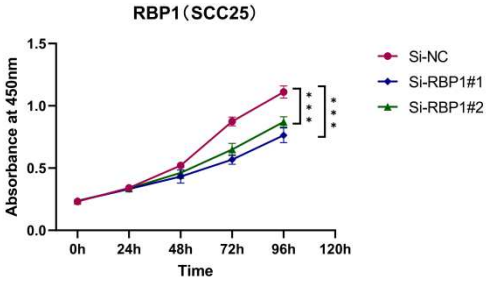


Fig.7 CCK-8 Assay Detecting the Effect of RBP1 Knockdown on Proliferative Capacity of HNSCC SCC-25 Cells. Compared with the si-NC (negative control) group, the proliferative capacity of SCC-25 cells was significantly attenuated in the si-RBP1#1 and si-RBP1#2 groups ($P < 0.001$).

(3) Effect of RBP1 Knockdown on Colony Formation Ability of SCC-25 Cells

Colony formation assay revealed that the colony formation ability of SCC-25 cells in the siRBP1 group was significantly attenuated compared with the si-NC group (Fig. 8, $P < 0.01$). These results demonstrate that RBP1 knockdown markedly suppresses the colony formation capacity of SCC-25 cells.

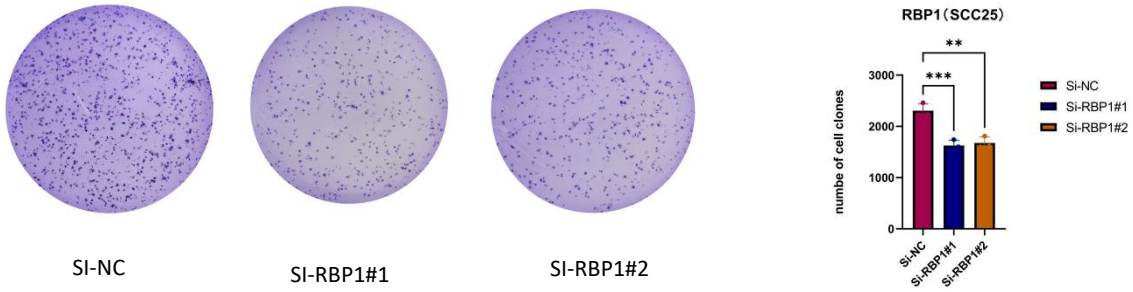


Fig.8 Colony Formation Assay Detecting the Effect of RBP1 Knockdown on Colony Formation Ability of SCC-25 Cells. Compared with the si-NC (negative control) group, the colony formation ability of SCC-25 cells was significantly attenuated in the si-RBP1#1 ($P < 0.001$) and si-RBP1#2 ($P < 0.01$) groups.

(4) Effect of RBP1 Knockdown on Migratory Capacity of SCC-25 Cells

Wound healing assay data demonstrated that microscopic examination of scratch closure at 24 hours post-wounding revealed significantly attenuated migratory capacity in SCC-25 cells of the siRBP1 group compared with the si-NC group (Fig. 9, $P < 0.001$).

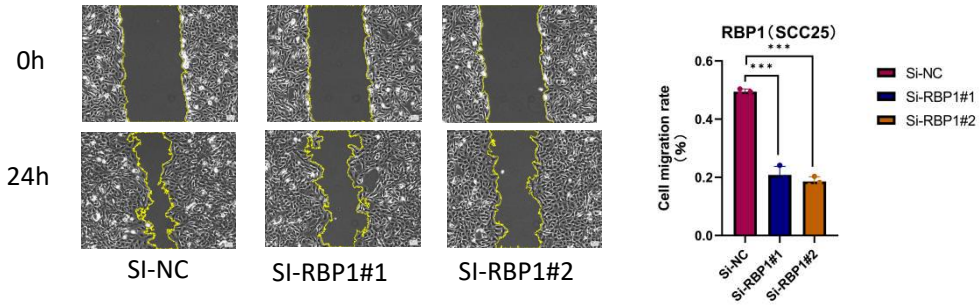


Fig.9 Wound Healing Assay Detecting the Effect of RBP1 Knockdown on Migratory Capacity of SCC-25 Cells. Compared with the si-NC (negative control) group, the migratory capacity of SCC-25 cells was significantly attenuated in the si-RBP1#1 and si-RBP1#2 groups ($P < 0.001$).

(5) Effect of RBP1 Knockdown on Invasive Capacity of SCC-25 Cells

Transwell invasion assay data demonstrated that the invasive capacity of SCC-25 cells in the siRBP1 group was significantly attenuated compared with the si-NC group (Fig. 10, $P < 0.01$).

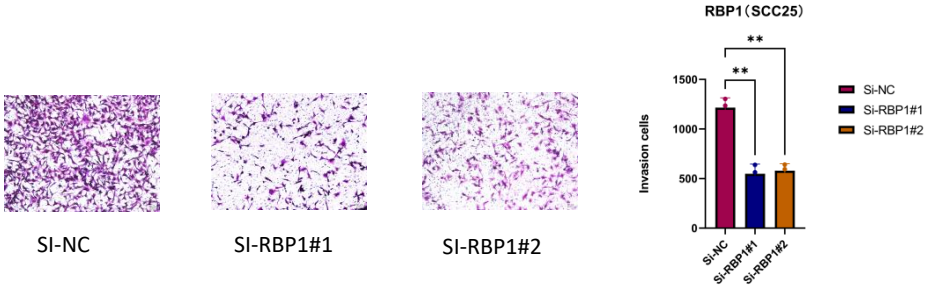


Fig.10 Transwell Invasion Assay Detecting the Effect of RBP1 Knockdown on Invasive Capacity of SCC-25 Cells. Compared with the si-NC (negative control) group, the invasive capacity of SCC-25 cells was significantly attenuated in the si-RBP1#1 and si-RBP1#2 groups ($P < 0.01$).

5.5.2 Effects of RBP1 Overexpression on Biological Functions of HNSCC Cell Lines

(1) Validation of RBP1 Overexpression and Transfection Efficiency

Following 24-hour transfection of SCC-9 cells, quantitative real-time polymerase chain reaction (qRT-PCR) was performed to assess RBP1 mRNA expression. The results demonstrated that RBP1 mRNA expression was significantly elevated in the pcDNA3.1-RBP1 group (transfected with pcDNA3.1-RBP1 overexpression plasmid) compared with the pcDNA3.1-NC group (transfected with pcDNA3.1 empty vector) (Fig. 11a, $P < 0.001$). Subsequently, SCC-9 cells were harvested at 48 hours post-transfection for Western blot analysis of RBP1 protein expression. The results confirmed that RBP1 protein levels were markedly increased in the pcDNA3.1-RBP1 group compared with the pcDNA3.1-NC group (Fig. 11b).

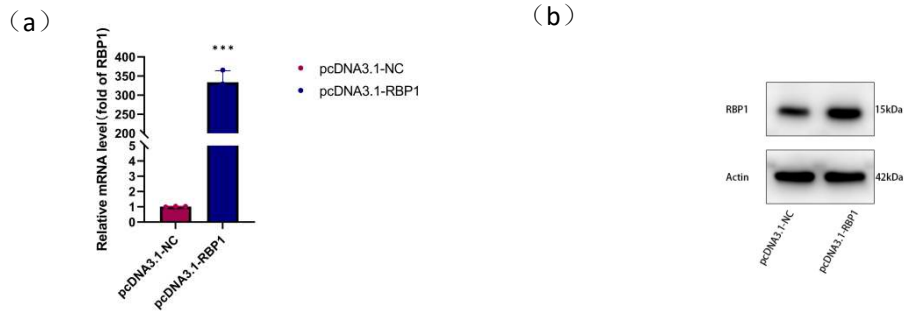


Fig.11 RBP1 Expression Following Overexpression in SCC-9 Cells.(a) Quantitative real-time polymerase chain reaction (qRT-PCR) detection of RBP1 mRNA expression following overexpression in SCC-9 cells. Compared with the pcDNA3.1-NC (negative control) group, RBP1 expression was significantly elevated in the pcDNA3.1-RBP1 group ($P < 0.001$).**(b)** Western blot analysis of RBP1 protein expression following overexpression in SCC-9 cells. β-actin served as the loading control.

(2) Effect of RBP1 Overexpression on Proliferative Capacity of SCC-9 Cells

Cell Counting Kit-8 (CCK-8) assay data demonstrated that the absorbance at 450 nm (A_{450}) of SCC-9 cells in the pcDNA3.1-RBP1 group was significantly elevated compared with the pcDNA3.1-NC group following 96-hour culture, with statistically significant differences observed (Fig. 12, $P < 0.001$). These results indicate that RBP1 overexpression promotes the proliferative capacity of HNSCC SCC-9 cells.

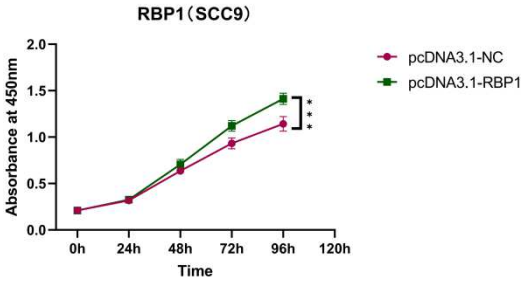


Fig.12 CCK-8 Assay Detecting the Effect of RBP1 Overexpression on Proliferative Capacity of HNSCC SCC-9 Cells. Compared with the pcDNA3.1-NC (negative control) group, the proliferative capacity of SCC-9 cells was significantly enhanced in the pcDNA3.1-RBP1 group ($P < 0.001$).

(3) Effect of RBP1 Overexpression on Colony Formation Ability of SCC-9 Cells

Colony formation assay revealed that the colony formation ability of SCC-9 cells in the pcDNA3.1-RBP1 group was significantly enhanced compared with the pcDNA3.1-NC group (Fig. 13, $P < 0.01$). These results demonstrate that RBP1 overexpression markedly promotes the colony formation capacity of SCC-9 cells.

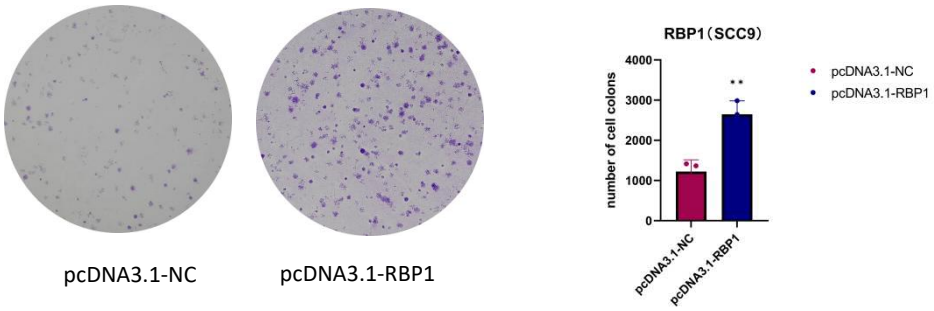


Fig.13 Colony Formation Assay Detecting the Effect of RBP1 Overexpression on Colony Formation Ability of SCC-9 Cells. Compared with the pcDNA3.1-NC (negative control) group, the colony formation ability of SCC-9 cells was significantly enhanced in the pcDNA3.1-RBP1 group ($P < 0.01$).

(4) Effect of RBP1 Overexpression on Migratory Capacity of SCC-9 Cells

Wound healing assay data demonstrated that microscopic examination of scratch closure at 24 hours post-wounding revealed significantly enhanced migratory capacity in SCC-9 cells of the pcDNA3.1-RBP1 group compared with the pcDNA3.1-NC group (Fig. 14, $P < 0.001$).

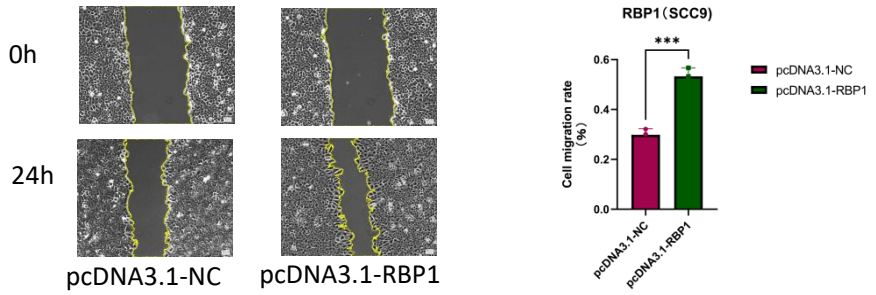


Fig.14 Wound Healing Assay Detecting the Effect of RBP1 Overexpression on Migratory Capacity of SCC-9 Cells. Compared with the pcDNA3.1-NC (negative control) group, the migratory capacity of SCC-9 cells was significantly enhanced in the pcDNA3.1-RBP1 group ($P < 0.001$).

(5) Effect of RBP1 Overexpression on Invasive Capacity of SCC-9 Cells

Transwell invasion assay data demonstrated that the invasive capacity of SCC-9 cells in the pcDNA3.1-RBP1 group was significantly enhanced compared with the pcDNA3.1-NC group (Fig. 15, $P < 0.01$).

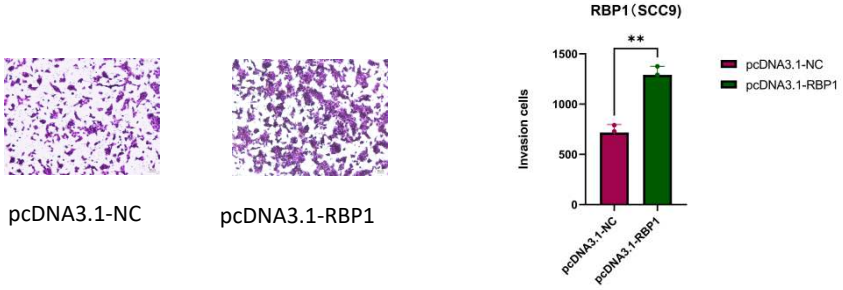


Fig.15 Transwell Invasion Assay Detecting the Effect of RBP1 Overexpression on Invasive Capacity of SCC-9 Cells. Compared with the pcDNA3.1-NC (negative control) group, the invasive capacity of SCC-9 cells was significantly enhanced in the pcDNA3.1-RBP1 group ($P < 0.01$).

6. Association Between RBP1 Expression and Paclitaxel Resistance in HNSCC

To investigate the clinical relevance of RBP1 in chemotherapeutic response, we analyzed overall survival outcomes of paclitaxel-treated HNSCC patients from the TCGA cohort using the Gene Expression Profiling Interactive Analysis 3 (GEPIA3) platform. Patients were stratified into high and low RBP1 expression groups based on the median expression value. Kaplan-Meier survival analysis revealed that the high RBP1 expression group exhibited significantly inferior overall survival compared with the low expression group ($P = 0.00266$, log-rank test) (Fig. 16a). The two survival curves demonstrated marked divergence within the first 20 months post-treatment, with the high RBP1 group showing precipitous decline in survival probability, whereas the low expression group maintained a relatively stable survival rate exceeding 75% at 40 months.

To complement this clinical observation, *in silico* prediction of paclitaxel sensitivity was performed using the pRRophetic package in R software (version 4.4.2) following model training. HNSCC samples were dichotomized based on RBP1 expression levels, with higher predicted values indicating enhanced drug sensitivity. Consistent with the survival data, high RBP1 expression samples exhibited significantly attenuated paclitaxel sensitivity compared with the low expression control group (Fig. 16b).

Collectively, these clinical and computational predictive findings establish RBP1 as a pleiotropic oncogenic driver in HNSCC—not only promoting malignant phenotypes including proliferation and metastasis (as substantiated by our functional assays), but also conferring therapeutic resistance to first-line chemotherapeutic agents. The convergent evidence from patient survival data and transcriptome-based drug sensitivity prediction underscores the clinical translational potential of targeting RBP1 to overcome treatment failure in HNSCC; however, these computational predictions remain to be experimentally validated.

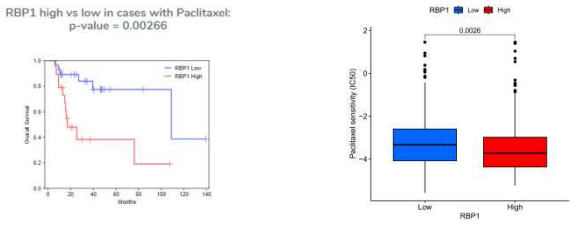


Fig.16 RBP1 Expression Is Associated with Paclitaxel Resistance and Poor Survival in HNSCC.(a) Kaplan-Meier overall survival analysis of paclitaxel-treated HNSCC patients from The Cancer Genome Atlas (TCGA) cohort (Gene Expression Profiling Interactive Analysis 3 [GEPIA3]), stratified by RBP1 expression levels. Patients were dichotomized into high and low RBP1 expression groups based on the median expression value. The high RBP1 expression group exhibited significantly inferior overall survival compared with the low expression group (P = 0.00266, log-rank test). Tick marks indicate censored data.**(b)** *In silico* prediction of paclitaxel sensitivity in HNSCC samples stratified by RBP1 expression levels, analyzed using the pRRophetic package in R software (version 4.4.2). Higher predicted values indicate enhanced drug sensitivity. High RBP1 expression samples demonstrated significantly attenuated paclitaxel sensitivity compared with low expression samples (P = 0.0026).

7. Immune Infiltration Analysis

Tumor immune infiltration analysis was performed using the Tumor Immune Estimation Resource (TIMER) database to evaluate RBP1-associated immune microenvironment landscapes in head and neck squamous cell carcinoma (HNSCC). The results demonstrated that RBP1 expression was significantly correlated with the infiltration levels and signature marker expression of multiple immune cell subsets, as visualized in Fig.17: B cells (Fig. 17a; CD19, CD79A, CD79B), CD4+ T cells (Fig. 17b; CD4), CD8+ T cells (Fig. 17c; CD8A, CD8B), dendritic cells (Fig. 17d; CD1C, HLA-DPA1, HLA-DPB1, HLA-DRA), M2 macrophages (Fig. 17e; CD163, MS4A4A), mast cells (Fig. 17f; CPA3, MS4A2, TPSB2), monocytes (Fig. 17g; CX3CR1, LYZ), tumor-associated macrophages (TAMs; Fig. 17h; CCL2), T follicular helper cells (Tfh; Fig. 17i; BCL6, IL21), T helper 1 cells (Th1; Fig. 17j; IFNG, STAT4, TBX21), T helper 2 cells (Th2; Fig. 17k; STAT5A, STAT6), as well as immune checkpoint molecules (Fig. 17l; CTLA4, HAVCR2, IDO1, LAG3, PDCD1, TIGIT). Notably, RBP1 exhibited a negative regulatory role in these immune interactions ($P < 0.05$).

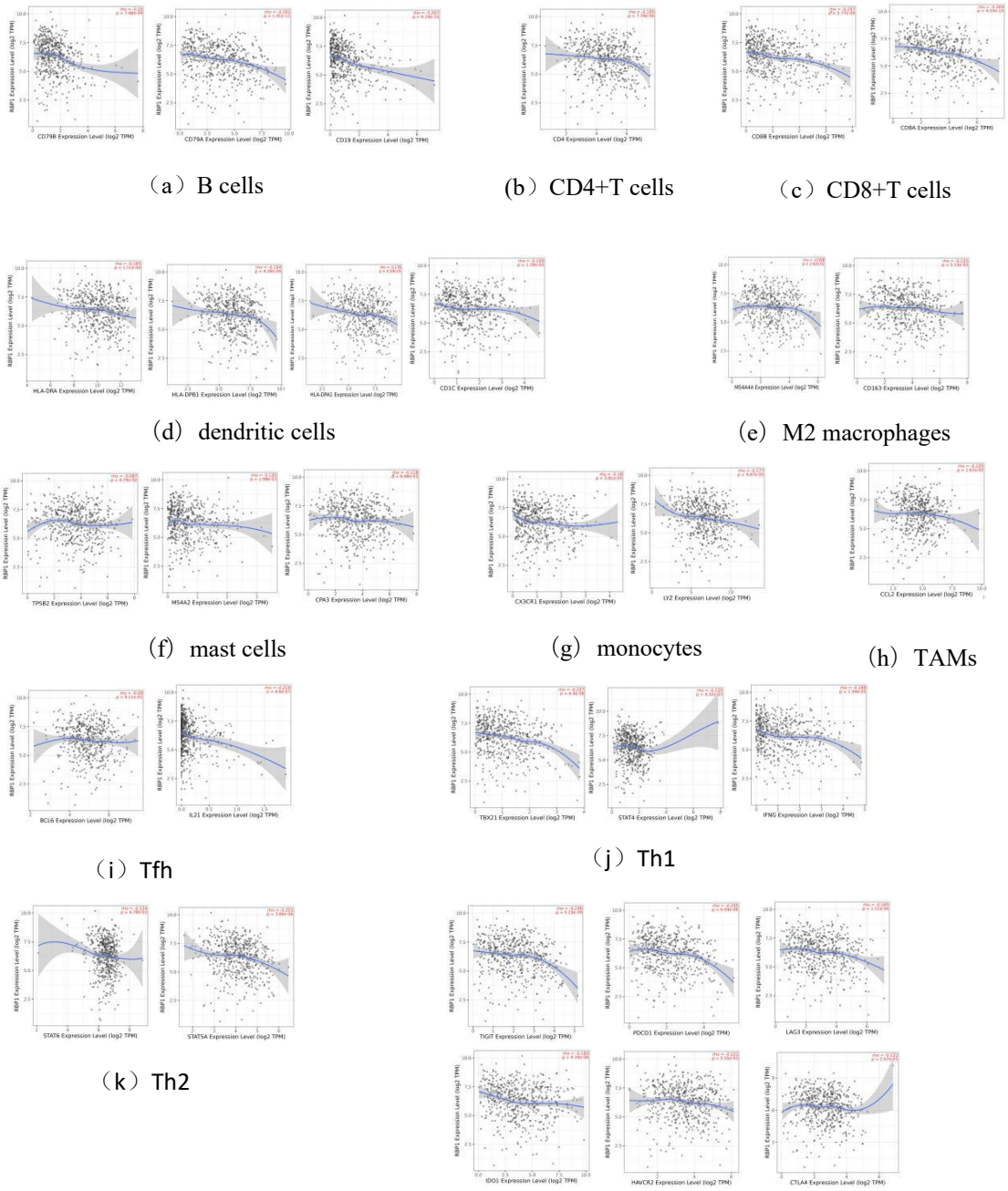


Fig.17 Correlation Scatter Plots of RBP1 Expression with Immune Infiltration in HNSCC Analyzed Using TIMER 2.0.(a) B cells (CD19, CD79A, CD79B); **(b)** CD4+ T cells (CD4); **(c)** CD8+ T cells (CD8A, CD8B); **(d)** dendritic cells (CD1C, HLA-DPA1, HLA-DPB1, HLA-DRA); **(e)** M2 macrophages (CD163, MS4A4A); **(f)** mast cells (CPA3, MS4A2, TPSB2); **(g)** monocytes (CX3CR1, LYZ); **(h)** tumor-associated macrophages (TAMs; CCL2); **(i)** T follicular helper cells (Tfh; BCL6, IL21); **(j)** T helper 1 cells (Th1; IFNG, STAT4, TBX21); **(k)** T helper 2 cells (Th2; STAT5A, STAT6); **(l)** immune checkpoint molecules (CTLA4, HAVCR2, IDO1, LAG3, PDCD1, TIGIT). All correlations are statistically significant ($P < 0.05$).

Discussion

1. Major Findings and Summary

In the present study, we systematically elucidated the aberrant expression pattern of cellular retinol-binding protein 1 (RBP1, also known as CRBP1) in head and neck squamous cell carcinoma (HNSCC) and its biological implications. First, RBP1 was significantly overexpressed in HNSCC cell lines and tumor tissues, and its elevated expression was closely associated with advanced T stage, regional lymph node metastasis (N stage), higher overall TNM stage, patient age, and unfavorable prognosis—suggesting the potential of RBP1 as a biomarker during HNSCC initiation and progression. Second, *in vitro* functional assays confirmed that RBP1 overexpression markedly promoted the proliferative, migratory, and invasive capacities of HNSCC cells, whereas RBP1 knockdown significantly attenuated these malignant phenotypes, substantiating the oncogenic role of RBP1 in HNSCC. Furthermore, analysis using the Tumor Immune Estimation Resource (TIMER) database revealed significant correlations between RBP1 expression and the HNSCC immune microenvironment, offering novel insights into RBP1-mediated tumor-immune interactions. Collectively, this study identifies the differential expression and pro-tumorigenic effects of RBP1, a critical regulator of vitamin A (retinol) metabolism, in HNSCC, further corroborates its detrimental impact on neoplastic cellular functions, and preliminarily explores its association with tumor immunity—providing a theoretical foundation for early diagnosis and targeted therapeutic strategies against HNSCC.

2. Expression Pattern and Clinical Significance of RBP1 in HNSCC

As a principal member of the retinol-binding protein family, cellular retinol-binding protein 1 (RBP1, also known as CRBP1) serves as the primary intracellular transporter of retinol and has traditionally been considered to exert tumor-suppressive effects by facilitating the conversion of retinol to retinoic acid [7]. However, accumulating evidence indicates that the functional role of RBP1 in malignancies exhibits remarkable tissue specificity. For instance, in prostate cancer, cervical cancer, and endometrial carcinoma, promoter hypermethylation-mediated silencing of RBP1 expression has been implicated in tumor progression, supporting its classification as a tumor suppressor gene [15][16][17]. Conversely, in lung adenocarcinoma, laryngeal squamous cell carcinoma, tongue squamous cell carcinoma, and the HNSCC investigated in the present study, RBP1 demonstrates aberrant overexpression and is associated with unfavorable prognosis—suggesting an oncogenic function in promoting tumor initiation and progression [18][19][20][12]. This heterogeneity in expression patterns may reflect differential reprogramming of retinoid metabolic pathways across distinct tumor tissues.

The positive correlation between elevated RBP1 expression and advanced N stage as well as higher overall TNM stage in HNSCC warrants particular attention. Lymph node metastasis represents a critical determinant of unfavorable prognosis in HNSCC patients [2][21], and RBP1 may promote metastatic dissemination by enhancing the migratory and invasive capacities of neoplastic cells. This finding was directly substantiated by our functional assays, wherein RBP1 overexpression significantly augmented the migratory and invasive capabilities of HNSCC cells ($P < 0.001$). Notably, TIMER database analysis revealed significant associations between RBP1 expression and tumor immune infiltration patterns, suggesting that RBP1 may indirectly influence the metastatic process through modulation of the tumor immune microenvironment. For instance, retinoic acid signaling has been documented to suppress dendritic cell maturation and promote the polarization of immunosuppressive macrophages; RBP1-mediated alterations in local retinoic acid metabolism may consequently reshape the tumor immune microenvironment, thereby creating a permissive niche conducive to tumor metastasis.

3. Molecular Mechanisms Underlying RBP1-Mediated Promotion of Malignant Phenotypes in HNSCC

Our functional assays unequivocally substantiated the positive regulatory role of RBP1 in HNSCC cell proliferation, migration, and invasion. This finding is consistent with the observations reported by Gao et al. [13] in oral squamous cell carcinoma (OSCC), wherein iTRAQ-based proteomic profiling identified RBP1 as a significantly upregulated protein, and the RBP1-CKAP4 axis was demonstrated to activate oncogenic autophagy. Autophagy, as a critical stress-responsive pathway, exhibits dichotomous roles in malignancies: basal autophagy exerts tumor-suppressive effects, whereas hyperactivated autophagy promotes tumor initiation and progression by supplying energy and eliminating damaged organelles [22][23]. RBP1 may modulate intracellular retinol metabolism, thereby influencing the activity of key autophagy-regulating kinases such as mammalian target of rapamycin (mTOR) and associated sensing pathways to fine-tune autophagic flux [24]. Beyond autophagy, RBP1 may promote HNSCC progression through multiple alternative mechanisms. Studies have demonstrated that in lung adenocarcinoma, RBP1 activates the Akt/Erk/EGFR signaling cascade [25], whereas in non-glioblastoma diffuse gliomas, it is associated with NF-κB pathway activation [26]. These signaling cascades are frequently activated in HNSCC and are intimately linked to therapeutic resistance [2][27][28][29][30]. Furthermore, retinoic acid signaling regulates cell cycle machinery, including cyclin D1 and cell cycle inhibitors such as p27^Kip1, through heterodimeric retinoic acid receptor/retinoid X receptor (RAR/RXR) complexes [31]. RBP1 overexpression may induce retinoic acid metabolic dysregulation, generating atypical retinoid signals that consequently abrogate normal cell cycle constraints.

The TIMER analysis results from the present study further suggest that RBP1 may participate in tumor immune evasion. Retinoic acid plays a pivotal role in immune cell differentiation, inducing regulatory T cell (Treg) differentiation while suppressing effector T cell function. RBP1-mediated elevation of local retinoic acid concentrations may enhance the immunosuppressive capacity of tumor cells—a hypothesis requiring validation through *in vitro* co-culture experiments and *in vivo* immunocompetent models.

4. The Vitamin A-RBP1 Axis: From Metabolic Regulation to Tumor Progression

The central innovative contribution of this study lies in establishing a direct association between vitamin A (retinol) metabolism and HNSCC progression. Conventional paradigms posit that vitamin A and its derivative retinoic acid exert tumor-suppressive effects through activation of retinoic acid receptor/retinoid X receptor (RAR/RXR) heterodimers—a theoretical foundation that has motivated extensive exploration of retinoid compounds as chemopreventive agents [5][6][7]. However, the suboptimal efficacy of retinoic acid in HNSCC prevention observed in clinical trials, coupled with the potential for paradoxical procarcinogenic effects, together with the oncogenic RBP1 effects documented in the present study, collectively illuminate the complexity of vitamin A metabolism in tumor pathobiology.

We propose the following speculative framework to reconcile this apparent paradox. In normal epithelial cells, moderate RBP1 expression maintains retinol homeostasis, facilitates retinoic acid biosynthesis, and thereby preserves the equilibrium between cellular differentiation and proliferation. In HNSCC, aberrant RBP1 overexpression induces dysregulated retinol metabolic flux [24][26], potentially engendering three principal consequences: (i) excessive local retinoic acid concentrations leading to RAR signaling desensitization or aberrant activation of non-canonical pathways [32][33]; (ii) accumulation of retinyl ester products that function as signaling lipids to activate PI3K/Akt or

mitogen-activated protein kinase (MAPK) cascades [34][35][36]; and (iii) compensatory upregulation of retinoic acid metabolic enzymes, potentially generating bioactive atypical retinoid derivatives. This "metabolic reprogramming" hypothesis aligns with the central tenet of contemporary tumor metabolism research: that altered expression of metabolic enzymes and transporters can rewire metabolic networks to generate bioactive metabolites that support neoplastic growth [37][38][39][40].

5. Therapeutic Potential of Targeting RBP1 in HNSCC

The clinical correlation analysis results from the present study provide a theoretical foundation for RBP1 as a therapeutic target in HNSCC. Current standard therapeutic modalities for HNSCC, including surgical resection, radiotherapy, and chemotherapy, are confronted with challenges such as high recurrence rates and substantial toxicities, whereas targeted therapeutic options remain limited, with cetuximab being the sole agent approved for recurrent/metastatic HNSCC [2][41][42]. Although RBP1, as an intracellular soluble protein, has traditionally been considered "undruggable," recent advances in developing small-molecule inhibitors, proteolysis-targeting chimera (PROTAC) degraders, and RNA interference-based strategies have furnished novel tools for targeting such proteins [43][44][45].

Notably, the potential association between RBP1 and immunotherapy warrants particular attention. TIMER analysis suggests significant correlations between RBP1 expression and immune infiltration patterns, while retinoic acid signaling has been documented to modulate programmed death-ligand 1 (PD-L1) expression and T cell functionality [46][47]. Consequently, combinatorial strategies simultaneously targeting RBP1 and immune checkpoints (e.g., PD-1/PD-L1) may engender synergistic antitumor effects [33][48][49]. Furthermore, given the pivotal role of RBP1 in vitamin A metabolism, the association between dietary vitamin A intake and HNSCC risk merits reevaluation; high-dose vitamin A supplementation in RBP1-high tumors may paradoxically exert procarcinogenic rather than tumor-suppressive effects [32][50][51].

6. Limitations and Future Directions

The present study is subject to several limitations. First, the findings are predominantly derived from *in vitro* cellular experiments and public database bioinformatics analyses, lacking validation in *in vivo* animal models. The construction of conditional RBP1 knockout or overexpression transgenic mouse models, or the utilization of patient-derived xenograft (PDX) models, would facilitate further substantiation of the oncogenic role of RBP1 in a physiologically relevant context.

Second, although TIMER database analysis suggests associations between RBP1 expression and immune infiltration, it fails to discriminate the specific contributions of distinct immune cell subsets and cannot establish causality. Single-cell RNA sequencing and spatial transcriptomics technologies would enable precise dissection of the relationship between RBP1 expression and the tumor immune microenvironment.

Third, the downstream molecular mechanisms through which RBP1 promotes HNSCC progression remain incompletely elucidated. The present study did not perform transcriptomic or proteomic profiling to identify RBP1 effector molecules. Future investigations should employ multi-omics approaches, including RNA sequencing (RNA-seq), chromatin immunoprecipitation sequencing (ChIP-seq), and metabolomics, to systematically delineate the signaling networks and metabolic pathways regulated by RBP1.

Fourth, the causal relationship between RBP1 and vitamin A metabolism requires more direct experimental evidence, such as isotope tracing experiments to monitor alterations in retinol metabolic flux following RBP1 overexpression or knockdown.

7. Conclusion

Collectively, this study reveals the aberrant overexpression of cellular retinol-binding protein 1 (RBP1, also known as CRBP1) in head and neck squamous cell carcinoma (HNSCC) and its intimate association with unfavorable patient prognosis. RBP1 may serve as a valuable biomarker for lymph node metastasis, and its oncogenic function in promoting HNSCC cell proliferation, migration, and invasion has been substantiated through *in vitro* functional assays. Furthermore, the significant correlation between RBP1 expression and the HNSCC immune microenvironment suggests its potential involvement in tumor immune modulation. These findings substantially challenge the conventional paradigm of retinol-binding proteins as merely tumor-suppressive factors, and implicate the vitamin A-RBP1 axis as a potentially novel driver mechanism underlying HNSCC progression. This work lays a preliminary foundation and offers novel opportunities for the development of precision therapeutic strategies targeting this metabolic-immune interactive axis.

Declarations

● Abbreviations

Abbreviation	Full Form
HNSCC	Head and Neck Squamous Cell Carcinoma
TME	Tumor Microenvironment
RBP1	Retinol-Binding Protein 1 (also known as CRBP1)
CRBP1	Cellular Retinol-Binding Protein 1
TCGA	The Cancer Genome Atlas
RNA-seq	RNA Sequencing
qRT-PCR	Quantitative Real-Time Polymerase Chain Reaction
IHC	Immunohistochemistry
siRNA	Short Interfering RNA
CCK-8	Cell Counting Kit-8
GEPIA	Gene Expression Profiling Interactive Analysis
TIMER	Tumor Immune Estimation Resource
T stage	Primary Tumor Size and Local Extent
N stage	Regional Lymph Node Metastasis
TNM	Tumor-Node-Metastasis
TAMs	Tumor-Associated Macrophages
Tfh	T Follicular Helper Cells
Th1	T Helper 1 Cells
Th2	T Helper 2 Cells
P	Probability
HR	Hazard Ratio
CI	Confidence Interval
AUC	Area Under the Curve
ROC	Receiver Operating Characteristic
OS	Overall Survival
PFA	Paraformaldehyde
PBS	Phosphate-Buffered Saline

FBS	Fetal Bovine Serum
DMEM	Dulbecco's Modified Eagle Medium
PVDF	Polyvinylidene Difluoride
ECL	Enhanced Chemiluminescence
BCA	Bicinchoninic Acid
TBST	Tris-Buffered Saline with Tween-20
ANOVA	Analysis of Variance
HSD	Honestly Significant Difference
SD	Standard Deviation
SEM	Standard Error of the Mean

● Ethics approval and consent to participate

This study was approved by the Ethics Committee of the Fourth Hospital of Hebei Medical University (Approval No. 2024KY180). Written informed consent was obtained from all participants or their legally authorized representatives.This study conforms to the principles of the Declaration of Helsinki.

● Consent for publication

Written informed consent for publication of clinical details was obtained from the patient.

● Availability of data and materials

The datasets analyzed in this study are publicly available from the following resources: The datasets generated and analyzed during the current study are available in the TCGA database.The Cancer Genome Atlas (TCGA) database (https://portal.gdc.cancer.gov/), Venny platform (https://bioinfogp.cnb.csic.es/tools/venny/), TIMER database (https://compbio.cn/timer2/), GEPIA database (https://gepia3.bioinfoliu.com/about/), and GeneCards database (https://www.genecards.org/). The RNA-seq expression data have been deposited in the National Genomics Data Center (NGDC) under accession number OMIX018823（https://share.cncb.ac.cn/Sn15lXFmJB/OMIX018823/）.

● Competing Interests

The authors declare no competing interests.

● Funding

This study was supported by the Medical Science Research Project of Hebei (Grant No. 20260512), the Central Government Guides Local Funds Supported by the S&T Program of Hebei (Grant No. 246Z7762G), the Traditional Chinese Medicine Program of Hebei Provincial Administration (Grant No. 2026349), and the Medical Science Research Project of Hebei (Grant No. 20250704).

● Authors' contributions

JZ and ZC were responsible for the conception and design of the study. JZ conducted the experiments and statistical analysis, and drafted the initial manuscript.JZ, TL,YL,HL,HS,BD, and TW made substantial revisions to important intellectual content. JZ,TL and MY performed English language editing. All authors contributed to the article and approved the final version submitted for publication.

● Acknowledgements

We extend our gratitude to the providers of the TCGA, TIMER, Venny platform, GEPIA, and GeneCards databases for making their valuable data resources accessible, facilitating the progression of this research.

References

[1] Sung, H, Ferlay, J, Siegel, RL, et al. Global Cancer Statistics 2020: GLOBOCAN Estimates of

Incidence and Mortality Worldwide for 36 Cancers in 185 Countries. CA Cancer J Clin. 2021; 71 (3): 209-249. doi: 10.3322/caac.21660

[2] Johnson, DE, Burtness, B, Leemans, CR, et al. Head and neck squamous cell carcinoma. Nat Rev Dis Primers. 2020; 6 Nat Rev Dis Primers. doi: 10.1038/s41572-020-00224-3

[3] Blomhoff, R, Blomhoff, HK. Overview of retinoid metabolism and function. J NEUROBIOL. 2006; 66 J NEUROBIOL. doi: 10.1002/neu.20242

[4] Zhong, M, Kawaguchi, R, Costabile, B, et al. Regulatory mechanism for the transmembrane receptor that mediates bidirectional vitamin A transport. P NATL ACAD SCI USA. 2020; 117 P NATL ACAD SCI USA. doi: 10.1073/pnas.1918540117

[5] Murillo, AG, Fernandez, ML. Potential of Dietary Non-Provitamin A Carotenoids in the Prevention and Treatment of Diabetic Microvascular Complications. ADV NUTR. 2016; 7 ADV NUTR. doi: 10.3945/an.115.009803

[6] Brown, G. Retinoic acid receptor regulation of decision-making for cell differentiation. Front Cell Dev Biol. 2023; 11 Front Cell Dev Biol. doi: 10.3389/fcell.2023.1182204

[7] Lavudi, K, Nuguri, SM, Olverson, Z, et al. Targeting the retinoic acid signaling pathway as a modern precision therapy against cancers. Front Cell Dev Biol. 2023; 11 Front Cell Dev Biol. doi: 10.3389/fcell.2023.1254612

[8] Ikeda, S, Truong, NB, Tran, AH, et al. Vitamin A Intake and Risk of Cancer Incidence: Insights from a Case-Control Study. Nutrients. 2025; 17 Nutrients. doi: 10.3390/nu17172744

[9] Sun, H, Kawaguchi, R. The membrane receptor for plasma retinol-binding protein, a new type of cell-surface receptor. INT REV CEL MOL BIO. 2011; 288 INT REV CEL MOL BIO. doi: 10.1016/B978-0-12-386041-5.00001-7

[10] Pierzchalski, K, Yu, J, Norman, V, et al. CrbpI regulates mammary retinoic acid homeostasis and the mammary microenvironment. FASEB J. 2013; 27 FASEB J. doi: 10.1096/fj.12-219410

[11] Li, H, Lei, Y, Li, S, et al. MicroRNA-20a-5p inhibits the autophagy and cisplatin resistance in ovarian cancer via regulating DNMT3B-mediated DNA methylation of RBP1. REPROD TOXICOL. 2022; 109 REPROD TOXICOL. doi: 10.1016/j.reprotox.2021.12.011

[12] Fu, LL, Yan, M, Yu, X, et al. Retinol-binding protein type 1 expression predicts poor prognosis in head and neck squamous cell carcinoma. BMC Cancer. 2024; 24 BMC Cancer. doi: 10.1186/s12885-024-12565-3

[13] Gao, L, Wang, Q, Ren, W, et al. The RBP1-CKAP4 axis activates oncogenic autophagy and promotes cancer progression in oral squamous cell carcinoma. Cell Death Dis. 2020; 11 Cell Death Dis. doi: 10.1038/s41419-020-2693-8

[14] Tsunoda, S, Smith, E, De Young, NJ, et al. Methylation of CLDN6, FBN2, RBP1, RBP4, TFPI2, and TMEFF2 in esophageal squamous cell carcinoma. ONCOL REP. 2009; 21 ONCOL REP. doi: 10.3892/or_00000325

[15] Cho, NY, Kim, BH, Choi, M, et al. Hypermethylation of CpG island loci and hypomethylation of LINE-1 and Alu repeats in prostate adenocarcinoma and their relationship to clinicopathological features. J PATHOL. 2007; 211 J PATHOL. doi: 10.1002/path.2106

[16] Mendoza-Rodriguez, M, Arreola, H, Valdivia, A, et al. Cellular retinol binding protein 1 could be a tumor suppressor gene in cervical cancer. Int J Clin Exp Pathol. 2013; 6 Int J Clin Exp Pathol. PMID: 24040446

[17] Orlandi, A, Ferlosio, A, Ciucci, A, et al. Cellular retinol binding protein-1 expression in endometrial hyperplasia and carcinoma: diagnostic and possible therapeutic implications.

MODERN PATHOL. 2006; 19 MODERN PATHOL. doi: 10.1038/modpathol.3800586

[18] Verusingam, ND, Yarmishyn, AA, Tsai, ML, et al. CircSPINT2 confers sensitivity to osimertinib via hsa-miR-1296-3p/RBP1 axis and inhibits NSCLC progression. Mol Ther Oncol. 2025; 33 Mol Ther Oncol. doi: 10.1016/j.omton.2025.201007

[19] Sun, M, Chen, S, Fu, M. Model establishment of prognostic-related immune genes in laryngeal squamous cell carcinoma. MEDICINE. 2021; 100 MEDICINE. doi: 10.1097/MD.0000000000024263

[20] Chen, Y, Tian, T, Mao, MJ, et al. CRBP-1 over-expression is associated with poor prognosis in tongue squamous cell carcinoma. BMC Cancer. 2018; 18 BMC Cancer. doi: 10.1186/s12885-018-4249-1

[21] van der Elst, A, Herrero-Saboya, D, Michon, L, et al. Molecular and immune landscape of recurrent and/or distant metastatic squamous cell carcinoma of the head and neck: an EORTC/IMMUCAN project. CLIN CANCER RES. 2026; CLIN CANCER RES. doi: 10.1158/1078-0432.CCR-25-3377

[22] Singh, SS, Vats, S, Chia, AY, et al. Dual role of autophagy in hallmarks of cancer. Oncogene. 2018; 37 Oncogene. doi: 10.1038/s41388-017-0046-6

[23] Yamamoto, K, Iwadate, D, Kato, H, et al. Targeting autophagy as a therapeutic strategy against pancreatic cancer. J GASTROENTEROL. 2022; 57 J GASTROENTEROL. doi: 10.1007/s00535-022-01889-1

[24] Doldo, E, Costanza, G, Agostinelli, S, et al. Vitamin A, cancer treatment and prevention: the new role of cellular retinol binding proteins. BIOMED RES INT. 2015; 2015 BIOMED RES INT. doi: 10.1155/2015/624627

[25] Doldo, E, Costanza, G, Ferlosio, A, et al. High expression of cellular retinol binding protein-1 in lung adenocarcinoma is associated with poor prognosis. Genes Cancer. 2015; 6 Genes Cancer. doi: 10.18632/genesandcancer.89

[26] Wu, W, Wang, Y, Niu, C, et al. Retinol binding protein 1-dependent activation of NF- κB signaling enhances the malignancy of non-glioblastomatous diffuse gliomas. CANCER SCI. 2022; 113 CANCER SCI. doi: 10.1111/cas.15233

[27] Li, C, Lin, X, Su, J. HSP90B1 regulates autophagy via PI3K/AKT/mTOR signaling, mediating HNSC biological behaviors. PeerJ. 2024; 12 PeerJ. doi: 10.7717/peerj.17028

[28] Liu, P, Kong, X, Yi, S, et al. IFIT3 accelerates the progression of head and neck squamous cell carcinoma by targeting PD-L1 to activate PI3K/AKT signaling pathway. World J Surg Oncol. 2024; 22 World J Surg Oncol. doi: 10.1186/s12957-023-03274-5

[29] Cai, F, Xu, H, Song, S, et al. Knockdown of Ubiquitin-Conjugating Enzyme E2 T Abolishes the Progression of Head and Neck Squamous Cell Carcinoma by Inhibiting NF-Kb Signaling and inducing Ferroptosis. CURR PROTEIN PEPT SC. 2024; 25 CURR PROTEIN PEPT SC. doi: 10.2174/0113892037287640240322084946

[30] Chai, F, Zhang, J, Fu, T, et al. Identification of SLC2A3 as a prognostic indicator correlated with the NF-κB/EMT axis and immune response in head and neck squamous cell carcinoma. CHANNELS. 2023; 17 CHANNELS. doi: 10.1080/19336950.2023.2208928

[31] Spinella, MJ, Freemantle, SJ, Sekula, D, et al. Retinoic acid promotes ubiquitination and proteolysis of cyclin D1 during induced tumor cell differentiation. J BIOL CHEM. 1999; 274 J BIOL CHEM. doi: 10.1074/jbc.274.31.22013

[32] Rossetti, S, Ren, M, Visconti, N, et al. Tracing anti-cancer and cancer-promoting actions of

all-trans retinoic acid in breast cancer to a RARα epigenetic mechanism of mammary epithelial cell fate. Oncotarget. 2016; 7 Oncotarget. doi: 10.18632/oncotarget.13500

[33] Esposito, M, Amory, JK, Kang, Y. The pathogenic role of retinoid nuclear receptor signaling in cancer and metabolic syndromes. J EXP MED. 2024; 221 J EXP MED. doi: 10.1084/jem.20240519

[34] Chen, Q, Zhang, K, Jiao, M, et al. Study on the Mechanism of Mesaconitine-Induced Hepatotoxicity in Rats Based on Metabonomics and Toxicology Network. Toxins (Basel). 2022; 14 Toxins (Basel). doi: 10.3390/toxins14070486

[35] Yue, S, Li, J, Lee, SY, et al. Cholesteryl ester accumulation induced by PTEN loss and PI3K/AKT activation underlies human prostate cancer aggressiveness. CELL METAB. 2014; 19 CELL METAB. doi: 10.1016/j.cmet.2014.01.019

[36] Muthusamy, T, Mukherjee, O, Menon, R, et al. A Method to Identify and Isolate Pluripotent Human Stem Cells and Mouse Epiblast Stem Cells Using Lipid Body-Associated Retinyl Ester Fluorescence. Stem Cell Reports. 2016; 7 Stem Cell Reports. doi: 10.1016/j.stemcr.2016.07.023

[37] Pavlova, NN, Thompson, CB. The Emerging Hallmarks of Cancer Metabolism. CELL METAB. 2016; 23 CELL METAB. doi: 10.1016/j.cmet.2015.12.006

[38] Vander Heiden, MG, DeBerardinis, RJ. Understanding the Intersections between Metabolism and Cancer Biology. CELL. 2017; 168 CELL. doi: 10.1016/j.cell.2016.12.039

[39] He, B, Li, L, Liu, Y, et al. BCAAs and related metabolic enzymes: partners in crime driving tumor development. FRONT CELL DEV BIOL. 2026; 14 FRONT CELL DEV BIOL. doi: 10.3389/fcell.2026.1748587

[40] Chiu, CF, Guerrero, JJG, Regalado, RRH, et al. Insights into Metabolic Reprogramming in Tumor Evolution and Therapy. Cancers (Basel). 2024; 16 Cancers (Basel). doi: 10.3390/cancers16203513

[41] Vermorken, JB, Mesia, R, Rivera, F, et al. Platinum-based chemotherapy plus cetuximab in head and neck cancer. NEW ENGL J MED. 2008; 359 NEW ENGL J MED. doi: 10.1056/NEJMoa0802656

[42] Bonner, JA, Harari, PM, Giralt, J, et al. Radiotherapy plus cetuximab for squamous-cell carcinoma of the head and neck. NEW ENGL J MED. 2006; 354 NEW ENGL J MED. doi: 10.1056/NEJMoa053422

[43] Burslem, GM, Crews, CM. Proteolysis-Targeting Chimeras as Therapeutics and Tools for Biological Discovery. CELL. 2020; 181 CELL. doi: 10.1016/j.cell.2019.11.031

[44] Sakamoto, KM, Kim, KB, Kumagai, A, et al. Protacs: chimeric molecules that target proteins to the Skp1-Cullin-F box complex for ubiquitination and degradation. P NATL ACAD SCI USA. 2001; 98 P NATL ACAD SCI USA. doi: 10.1073/pnas.141230798

[45] Setten, RL, Rossi, JJ, Han, SP. The current state and future directions of RNAi-based therapeutics. NAT REV DRUG DISCOV. 2019; 18 NAT REV DRUG DISCOV. doi: 10.1038/s41573-019-0017-4

[46] Li, T, Fan, J, Wang, B, et al. TIMER: A Web Server for Comprehensive Analysis of Tumor-Infiltrating Immune Cells. CANCER RES. 2017; 77 CANCER RES. doi: 10.1158/0008-5472.CAN-17-0307

[47] Li, T, Fu, J, Zeng, Z, et al. TIMER2.0 for analysis of tumor-infiltrating immune cells. NUCLEIC ACIDS RES. 2020; 48 NUCLEIC ACIDS RES. doi: 10.1093/nar/gkaa407

[48] Cao, D, Qi, Z, Pang, Y, et al. Retinoic Acid-Related Orphan Receptor C Regulates Proliferation,

Glycolysis, and Chemoresistance via the PD-L1/ITGB6/STAT3 Signaling Axis in Bladder Cancer. CANCER RES. 2019; 79 CANCER RES. doi: 10.1158/0008-5472.CAN-18-3842

[49] Ma, ZL, Ding, YL, Jing, J, et al. ATRA promotes PD-L1 expression to control gastric cancer immune surveillance. EUR J PHARMACOL. 2022; 920 EUR J PHARMACOL. doi: 10.1016/j.ejphar.2022.174822

[50] Mayne, ST, Cartmel, B, Baum, M, et al. Randomized trial of supplemental beta-carotene to prevent second head and neck cancer. CANCER RES. 2001; 61 CANCER RES. PMID: 11245451

[51] van Zandwijk, N, Dalesio, O, Pastorino, U, et al. EUROSCAN, a randomized trial of vitamin A and N-acetylcysteine in patients with head and neck cancer or lung cancer. For the EUropean Organization for Research and Treatment of Cancer Head and Neck and Lung Cancer Cooperative Groups. JNCI-J NATL CANCER I. 2000; 92 JNCI-J NATL CANCER I. doi: 10.1093/jnci/92.12.977

Supplementary Files

This is a list of supplementary files associated with this preprint. Click to download.

- 1RNAseq.xlsx